REPORT ON THE SCIENCE COORDINATION GROUP ACTIVITIES FOR THE JOINT DARK ENERGY MISSION (JDEM)

Neil Gehrels
Goddard Space Flight Center
Science Coordination Group Chair

April 10, 2009

Executive Summary

JDEM is a space-based observatory designed to perform precision measurements of the nature of dark energy in the Universe. The JDEM Science Coordination Group (SCG) was formed in September 2008 by NASA and DOE to bring the community together to define the top-level requirements and capabilities for a Reference Mission for the mission in coordination with the JDEM Project Office. This report presents the activities and results of the SCG, the level 1 and 2 requirements for progress in dark energy research and the Reference Mission configuration.

Key areas of discussion and conclusions reached by the SCG and were as follows:

1. The SCG was charged to consider a space mission incorporating three probes of dark energy onboard: baryon acoustic oscillations (BAO), supernovae (SNe) and weak lensing (WL). JDEM can accommodate these three techniques for progress on dark energy understanding. The techniques give different and complementary information on dark energy and its evolution. They provide cross checks on dark energy results that will be important for such precision measurements in cosmology.

2. Space observations provide unique capabilities needed for progress in dark energy research. These include wide-field photometry and spectroscopy, good resolution and dark background above the scintillating atmosphere, excellent systematic error control in the stable environment of L2, and round-the-clock full-sky survey measurement capability using well-characterized and stable instrumentation.

3. The Reference Mission developed by the Project Office has a 1.5m aperture with a visible CCD instrument and near infrared HgCdTe instrument. The near infrared instrument has an imager channel behind a filter wheel that covers 0.95 - 2.0 μm. It also has a slitless spectrometer channel with fixed prisms that covers 1.1 - 2.0 μm. The visible instrument has a filter wheel that covers 0.4 - 1.0 μm.

4. The JDEM Reference Mission offers more than an order of magnitude improvement in the Dark Energy Task Force (DETF; Albrecht et al. 2006) figure of merit (FoM) compared to Stage II experiments, which was a goal put forward by the DETF. Compared to pre-JDEM experiments as defined by the FoM Science Working Group (FoMSWG; Albrecht et al. 2009), it offers factor of 7-9 and 23-130 improvements for the DETF FoM (Albrecht et al. 2006) and the γ parameter, respectively. For other figures of merit defined by the FoMSWG the improvements are order of magnitude or larger.

5. JDEM combines ground-breaking capabilities for the three techniques:
- <u>BAO</u>: BAO measurement to within a factor of two of the cosmic variance limit in the $0.7<z<2$ range via a wide-field NIR survey. Redshifts and positions of $\sim 2 \times 10^8$ emission-line galaxies will be obtained in the 1.1-2 micron band. This BAO 3-D survey will provide a robust measurement of $D_A(z)$ and the valuable direct $H(z)$ that depends only on the geometry of galaxy separations.

- Supernovae: Photometric and spectroscopic observations of Type Ia Supernovae (SNe Ia) between $0.3 < z < 1.2$ in the near infrared enabling a reduction in systematic uncertainties by correcting for host galaxy dust properties and intrinsic supernovae properties, which, when combined with ground-based surveys at lower redshift, will provide precise determination of the luminosity distance $D_L(z)$
- WL: Wide-field WL survey with low-systematic-error shape measurements above the atmosphere, space-unique NIR filters for photometric redshift determination and a uniquely deep galaxy redshift survey through the NIR to calibrate the photometric redshift scale. Galaxy shape and redshifts of 1-2 x 10^9 galaxies will provide measurements of the growth of gravitational fluctuations over cosmic history, the bias of galaxies, and the cosmic expansion history.

6. A reference observing program of 6-7 years duration provides WL and BAO sky surveys with 10,000 and 20,000 square degree coverage, respectively, and SN monitoring over a few square degrees to give ~1000 SN Ia detections. The JDEM data must be supplemented with ground data to provide precision photometry in visible filters for the WL photo-z measurements and for lightcurves of low redshift SNe. The Reference Mission is capable of obtaining these data, but would require additional observing time. It is expected to be less expensive to obtain these data from careful ground-based observations.

7. The JDEM Reference Mission is enabled by now-available large-format CCD and HgCdTe detectors, wide-field broad-band diffraction-limited telescopes and ground high-speed processing and storage of large data sets. All JDEM technologies are at high Technology Readiness Level (TRL) and ready-to-go for space flight. JDEM can be built today.

Outline

I. SCG Charge and Membership

The Joint Dark Energy Mission (JDEM) Science Coordination Group (SCG) was constituted by NASA and DOE in September 2008 to aid in establishing preliminary requirements for JDEM and evaluating Reference Mission (RM) concepts for the mission produced by the JDEM Project Office (PO). Members on the SCG were selected via an open "Dear Colleague" letter and are as follows:

JDEM SCG Membership

Dominic Benford	Goddard Space Flight Center
Chuck Bennett	Johns Hopkins University
Gary Bernstein	University of Pennsylvania
Susana Deustua	Space Telescope Science Institute
Dan Eisenstein	University of Arizona
Richard Ellis	Caltech
Karl Gebhardt	University of Texas - Austin
Neil Gehrels (Chair)	Goddard Space Flight Center
Chris Hirata	Caltech
Bob Kirshner	Harvard-Smithsonian Center for Astrophysics
Tod Lauer	National Optical Astronomy Observatory
Gary Melnick	Harvard-Smithsonian Center for Astrophysics
Harvey Moseley	Goddard Space Flight Center
Saul Perlmutter	University of California Berkeley
Adam Riess	STScI, Johns Hopkins University
David Schlegel	Lawrence Berkeley National Laboratory
Yun Wang	University of Oklahoma

The SCG was charged with the following tasks:

1) Determine the top-level science and observational preliminary observational requirements and instrumentation capabilities for a JDEM mission using the science performance measures from the FoM SWG, incorporating at a minimum the Baryon Acoustic Oscillation (BAO), Supernova (SN) and Weak Lensing (WL) techniques.

2) Evaluate the science performance of an initial RM, provided by the JDEM PO, using the BAO, SN and WL techniques. The SCG should consider whether additional techniques should be included to enhance the science performance of the RM, within programmatic constraints.

3) Provide advice to the JDEM PO on the configuration of the RM to optimize the mission's science return consistent with programmatic constraints.

4) Devise a reference observing program as an example of how the RM can be used to meet requirements and achieve progress in dark energy understanding.

5) Obtain community input of JDEM. This was done with a web site open for comment. The comments submitted are compiled on the JDEM SCG web site (http://jdem.gsfc.nasa.gov/scg.html).

II. JDEM Programmatic Development

The discovery that the expansion of space is accelerating was described in 1998 by the journal Science as the breakthrough of the year and one of the most important scientific problems of our time. The implication that three quarters of the mass-energy in the Universe is due to an unknown entity, called "dark energy", may revolutionize our understanding of cosmology and physics when this phenomenon is fully characterized through further empirical study. Observations with ground-based and orbital assets, including HST, Chandra, and WMAP have confirmed the acceleration. However, to make a further major step forward in this critical area of new physics, a special purpose space-based experiment is needed.

Several prominent scientific advisory committees have evaluated the need for a dark energy space mission and each has concluded that it is necessary to advance this key area. The National Research Council's 2003 report, *Connecting Quarks with the Cosmos, Eleven Science Questions for the New Century* stressed the importance of a space-based dark energy mission. The Interagency Working Group (IWG) on the Physics of the Universe (IWG) was chartered by the National Science and Technology Council's Committee on Science. The IWG completed its report: *A 21st Century Frontier of Discovery: The Physics of the Universe; A Strategic Plan for Federal Research at the Intersection of Physics and Astronomy*, during 2004 with the recommendation that "NASA and DOE will develop a Joint Dark Energy Mission (JDEM) to be launched by the middle of the next decade." The Astronomy and Astrophysics Advisory Committee (AAAC) and the High Energy Physics Advisory Panel (HEPAP) established a Dark Energy Task Force (DETF) as a joint sub-committee to advise the DOE, NASA, and NSF on future dark energy research. The DETF reviewed all of the experimental methods for studying dark energy, developed a metric-based approach to assess the effectiveness of future dark energy experimental designs, and made a recommendation that Stage IV experiments, including JDEM, will be most powerful if more than one method is enabled (Albrecht et al. 2006). In 2007, the National Research Council's Beyond Einstein Program Assessment Committee (BEPAC) recommended (based on scientific importance and technical readiness) that JDEM be the first of NASA's Beyond Einstein Program mission to fly.

Against the background of the above findings, NASA issued open solicitations for dark energy mission concepts during 2003 and 2006 to aid NASA and DOE in their planning. These studies were completed in September 2008. To further develop the above DETF metrics for assessment of experimental methods, NASA commissioned an ad hoc JDEM

Figure of Merit Science Working Group (FoMSWG) during July 2008. This group re-examined the science goals of a space-based dark energy mission and developed metrics for its evaluation. The FoMSWG delivered its report (Albrecht et al. 2009) and analysis tools in December 2008. In Fall 2008, NASA and DOE announced plans for developing JDEM as an agency strategic mission with a NASA Announcement of Opportunity (AO) solicitation for JDEM science investigations. Project Offices were formed to develop the mission.

To enable the above AO solicitation, NASA and DOE formed a Science Coordination Group (SCG) in October 2008 with membership chosen competitively via solicited proposals. The task of the SCG was specified as defining the scientific requirements of JDEM and evaluating Reference Mission candidates developed by the Project Office. The boundary conditions laid out by the agencies were that the mission be in the NASA medium class and that three experimental methods (weak lensing, supernovae, baron acoustic oscillations) be combined onboard for maximal progress in dark energy understanding. This RM is also a conceptual level point of departure for a phase A mission study that will begin during 2009.

III. JDEM Techniques for Dark Energy Investigation

The DETF (Albrecht et al. 2006) and FoMSWG (Albrecht et al. 2009) identified 3 goals for JDEM as follows:

1. Determine as well as possible whether the accelerating expansion is consistent with a cosmological constant, i.e., unevolving dark-energy density,
2. Measure as well as possible any time evolution of the dark energy density,
3. Search for a possible failure of general relativity through comparison of the effect of dark energy on cosmic expansion with the effect of dark energy on the growth of cosmological structures.

They also found that three measurement techniques are particularly promising for progress on dark energy research with JDEM, namely Baryon Acoustic Oscillations, Type Ia Supernovae and Weak Lensing.

Many of the JDEM measurements are likely to be limited by systematic errors. The purpose of JDEM is to extend ground-based measurements of dark energy to the $z>1$ and obtain increased precision with a minimum of systematic errors over the full available redshift range. Here we describe the 3 primary measurement technique that JDEM will employ plus summarize several other promising techniques.

A. Baryon Acoustic Oscillations (BAO)

All of the structure in the Universe observed today was initially seeded by primordial density fluctuations in the early Universe. Initial regions of over-density were also regions of greater than average pressure which drove the expansion of spherical sound

waves. In particular, photons, electrons, and the baryon gas behaved as a single fluid until the expansion and cooling of the Universe reached the epoch of decoupling, leaving an extra abundance of baryons in spherical shells around the initially over-dense regions. The cosmic microwave background (CMB) photons free streamed away. The sky is filled with these spherical shells of baryons with fixed radii at decoupling of 148 Mpc, corresponding to the size of the horizon at decoupling. The power spectrum of the map shows the series of oscillatory peaks and troughs from these baryon acoustic oscillations.

WMAP provided the BAO calibration (Bennett et al. 2003; Komatsu et al. 2009), and future calibration improvements will come from the Planck mission. This established a "standard ruler" against which the Universe can be measured (Eisenstein & Bennett 2008). The shells of gas around the initial over-dense locations enhance the probability that galaxies formed with separations on the BAO scale. In 2005, the expected ~ 1% excess galaxy correlation was observed at the expected scale (Eisenstein et al. 2005).

Because galaxy correlations are enhanced by only 0.01 at the BAO scale, the use of BAO to probe dark energy requires that accurate redshifts and position of large numbers of galaxies be observed over large regions of the sky. Observations of the spherical sound waves are possible both along the line-of-sight and transverse to the line of sight. The transverse measurement requires the two-dimensional positions of galaxies. This is especially useful if there is information about the redshifts of the same galaxies.

Taking the tangential co-moving size as the sound horizon at decoupling, measured by the CMB, the tangential BAO measurements result in a measure of the angular diameter distance. The angular diameter distance is robustly based on the geometry between the observer and the horizon. This provides a distance similar to that of Type Ia supernovae but based on different physical processes. It has fewer known systematics and good statistics at $z>1$. At low redshifts, where there is insufficient cosmic volume for the BAO to achieve strong constraints and nonlinear effects become significant, the supernovae are singularly invaluable. The power of BAO dark energy measurements increases with redshift.

Taking the co-moving size as the sound horizon, the radial BAO gives the most precise direct measurement of the expansion rate $H(z)$. Also, the BAO measurements require only spectroscopic galaxy redshifts and positions, two of the least demanding and best established measurements in astrophysics.

JDEM will dwarf previous galaxy redshift surveys by measuring over a hundred million galaxy redshifts. The wide-field spectrometer will simultaneously disperse the light from all of the galaxies in the field of view, providing redshifts from the bright H-α spectral line. Galaxy positions will also be accurately determined. The resulting catalogue of three dimensional galaxy positions (α, δ, z) will then be used to determine the angular diameter distance, the expansion rate and the galaxy redshift distortions - all as functions of redshift. The latter probes the growth of structure to test gravity theory. The angular diameter measurement and the expansion rate measurement form a built-in check of

systematic errors. The Alcock-Paczynski (1979) test provides an additional cross-check. Comparison with weak lensing measurements is another cross-check.

JDEM enables a large advance over ground-based BAO surveys in two key ways:

1. Space NIR measurements have ~1000 times less background than those from the ground which must contend with the bright atmosphere. Broad-band, sensitive NIR coverage, which is uniquely available from space, enables a galaxy survey using the H-α spectral line in the $0.7 < z < 2$ range. This provides a greatly expanded cosmic volume for BAO observations compared to that available from the ground.
2. A space mission gives nearly uniform coverage over a large part of the sky with tight systematics control. JDEM can perform a redshift survey of 2×10^8 galaxies and harvest the full available BAO information to within a factor of 2 of the cosmic variance limit.

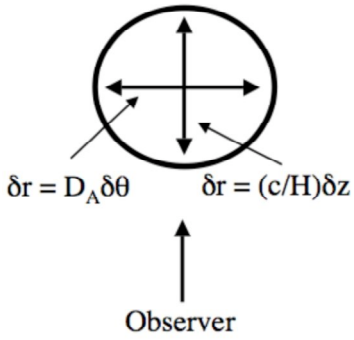

Figure 1: Cartoon of BAO spherical shell with H(z) and $D_A(z)$ measurements

B. Type Ia Supernovae (SNe)

Type Ia supernovae are believed to be the explosive disintegrations of a white dwarf star in a binary system that accretes material in excess of its Chandrasekhar stability limit of 1.38 solar masses. Because the progenitor masses of such supernovae are nearly all the same, the total energy released is expected to be the same (around 10^{44} Joules), and thus they offer the potential of providing excellent standard candles. For a known supernova luminosity L_{SN}, and measured flux F, the relation $F = L_{SN}/4 \quad D_L^2$ can be used to calculate the luminosity distance D_L directly. Certain spectral features in the supernova light may be used to identify the redshift, thereby providing a primary observable of the effect of dark energy: the distance-redshift relation $D(z)$.

The acceleration of the Universe was initially discovered using Type Ia supernovae observations at redshifts ($z \leq 0.9$). More recently, SNe observed from the Hubble Space

Telescope (HST) have been employed to observe the transition from an initially matter-dominated Universe to the present dark energy dominance at redshifts beyond $z = 1$, (see figure 10 from Kowalski et al. 2008, below). The SN technique currently shows a dark-energy signal with strong statistical significance and has advanced several generations beyond the original detection. It is thus a mature method with well developed study of systematics. This allows a JDEM mission to be designed that specifically targets the systematics to bring them below the statistical uncertainties. These include the effects of reddening, a variation of the luminosity with the rest-frame duration of the event (referred to as the light curve correction), and the variations in luminosity that depends on other properties of the SN or its host galaxy. It is believed that the variations in luminosity can be correlated with other, distance-independent, features of the supernova light curve, spectrum, or host galaxy. Thus Type Ia SNe are standardizable, to a high, systematics-limited degree of precision. This standardization process is empirical, and for JDEM will rely on having well-sampled light curves and spectra, and with sufficient numbers of events that subsampling for comparison and the estimation of systematic errors from various effects can be examined.

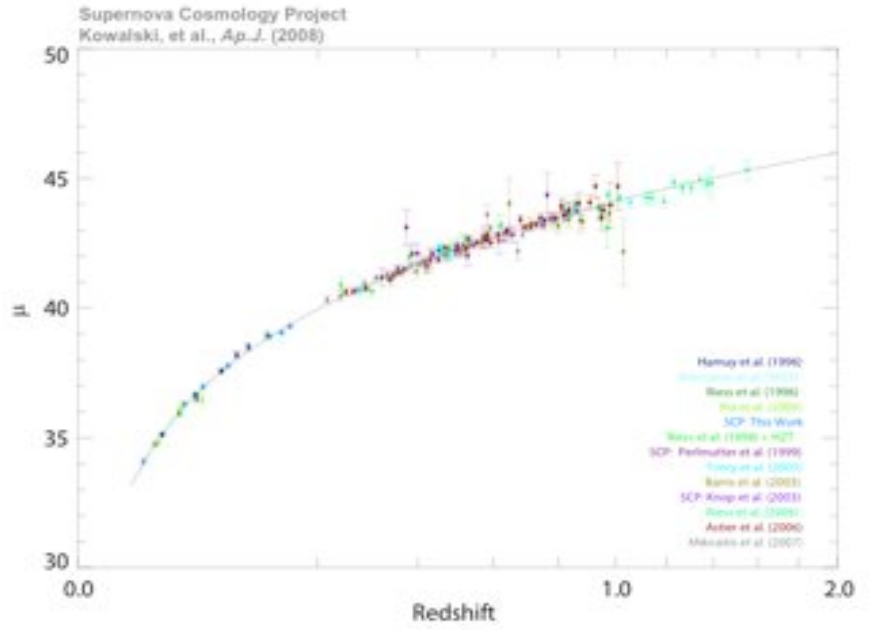

Figure 2: The Hubble diagram for SN Ia observations from the ground and space (HST). Plotted is the distance moduls, μ = apparent magnitude - absolute magnitude as a function of redshift.

JDEM will measure the properties of 750-1500 supernovae (range covers uncertainty in SN rates). A regular cadence of ≤5 days will sample the light curve of all supernovae to provide for correction, while spectroscopy provides simultaneous typing, redshift determination, and other spectral information. Observations covering the visible through

near-infrared (0.38-2.0 μm) permit a significant overlap of the entire rest-frame visible light in both photometry and spectroscopy for all events, regardless of redshift.

JDEM enables a large advance over ground-based SN surveys in five ways:

1. The low background and high efficiency of a wide-field imaging space telescope permit rapid monitoring of a large number of z~1 galaxies to find and follow many more supernovae than can readily be discovered from the ground. As redshifts increase past z ~0.8, discovery of SN become increasingly difficult form the ground.
2. The low NIR background, compact PSF, plus weather–free space environment offers high signal-to-noise observations with superior photometric accuracy
3. The light curves of SNe can be acquired in a homogeneous, gap-free manner since the space environment has no cloudy or moonlit periods.
4. Spectroscopy in the near-infrared can process spectra in the rest-frame visible at redshifts higher than would be possible from the ground, permitting accurate typing, redshift derivation, and tracking of spectral features around the time of peak light. Such spectral features can yield intrinsically lower dispersion in the final Hubble diagram and SN Ia subset comparisons to test evolution systematics.
5. Photometry in the rest-frame infrared, available to JDEM, has been found to yield intrinsically lower dispersion in the final Hubble diagram as compared to photometry in the rest-frame visible.

C. Weak Lensing (WL)

Traditional astronomy exploits the fact that photons arrive at Earth bearing information about the conditions of their origin in distant objects. As photons travel to Earth along the null geodesics of spacetime, WL exploits the fact that photons arrive carrying information about the geometry of spacetime *between* the source and Earth. Fluctuations in the gravitational potential(s) of space cause subtle distortions and magnification of the images of distant sources. In WL, these distortions are measured to infer the mass-density fluctuations that cause them, and the laws of gravity that relate the mass to the metric. WL determines the three dimensional total matter distribution in the Universe to infer the distance-vs-redshift relation, and hence the effect of dark energy on the expansion.

A crucial aspect of the WL method is its ability to provide a robust and precise measure of the growth of gravitational fluctuations over the history of the Universe. This enables a critical test of whether the cosmic acceleration is due to an unseen "dark energy" field, or, if instead it might be some failure of general relativity. The combination of WL data with the galaxy maps produced by a BAO experiment enables tests of several aspects of general relativity.

JDEM will detect WL by measuring the coherent distortion ("shear") of the images of distant galaxies. Because galaxies come in a variety of intrinsic shapes, it is not possible

to tell whether a single galaxy is gravitationally distorted. But lensing causes galaxies on similar lines of sight to align, so averaging large samples of galaxies can effectively map the lensing distortions. The signal is quite subtle: a 1–2% stretch of galaxy images along a typical line of sight. A reliable detection of "cosmic shear" requires $>10^5$ galaxy images. Such samples were not available until the advent of CCD mosaic cameras in the late 1990's; a flurry of cosmic-shear detections were published in 2000–2001. Current WL surveys image a few $\times 10^6$ galaxies over <200 deg^2 and measure key cosmological parameters to ~ 5% accuracy. At the launch of JDEM, we expect WL surveys will be underway to measure ~ 2×10^8 galaxies over ~ 5000 deg^2.

JDEM enables advances over ground-based WL surveys in four ways:

1. The low sky background, high efficiency, and high angular resolution of a wide-field imaging space telescope speed up the measurement of galaxy shapes, so that JDEM can measure $1–2 \times 10^9$ galaxy shapes, reducing statistical errors substantially.
2. Ground-based attempts to measure the subtle WL shape distortions to high accuracy are hindered by the image distortions induced by atmospheric fluctuations, plus thermal and gravitational distortions of the telescope optics. Ground-based experiments are limited by systematic errors in trying to distinguish these instrumental effects from true cosmic lensing. The exceptionally sharp and stable optical performance of a space telescope permit this systematic to be reduced and accurately removed.
3. The lensing survey requires accurate galaxy redshifts. This is essential to map the cosmic evolution of gravity, and to distinguish true cosmic lensing shear from any tidal alignment of neighboring galaxies. It is infeasible to obtain spectroscopic redshifts for 10^9 galaxies, so all WL surveys rely on *photometric redshifts*. The photo-z reliabilities needed for JDEM-quality WL experiments require deep, wide-field, NIR photometric surveys, which are feasible only from space.
4. The photometric redshift scale must be calibrated using very complete spectroscopic redshift survey of 30,000 –100,000 galaxies. The unique wide-field spectroscopic capabilities on JDEM will make this possible by measuring galaxy emission lines in redshift ranges that are inaccessible from the ground.

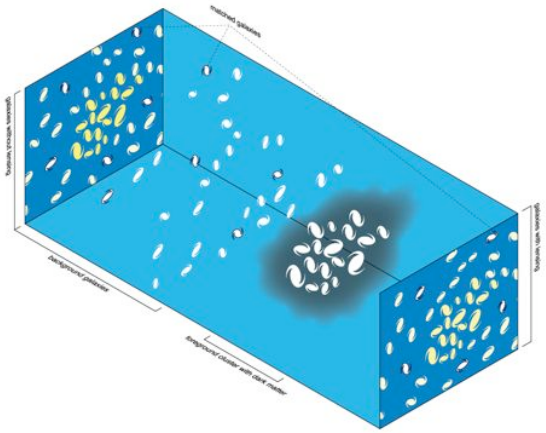

Figure 3: Illustration of Weak Lensing technique

D. Other Dark Energy Measurement Techniques

There are several other DE measurement techniques that the SCG discussed and are briefly documented here. In some cases, the current JDEM Reference Mission will be able to use the technique to extend the DE capabilities of the mission, while others could not be accommodated.

Alcock-Paczynski Test

The Alcock-Paczynski test (Alcock & Paczynski 1979) is based on the fact that a spherical object in real space will appear non-spherical (either prolate or oblate) in redshift space. For BAO, the radial size of the object is given by $\Delta z/H(z)$ and the transverse size if given by $d_{A(z)}$. By setting these two quantities equal, we can check the consistency of the independent measurements with the cosmology. The object can be the "bump" in the two-point correlation function, or cluster halos (which should be spherical over a large sample average). The Alcock-Paczynski test can show when the radial and tangential horizon sizes differ, or their relative expansion rates differ. This is an additional independent test of dark energy and cosmic consistency.

Large-Scale Isotropy

The WMAP CMB data, combined with other cosmological data, such as the SDSS galaxy redshift survey BAO data, provides the tightly constrained standard model of cosmology. While the Λ CDM model is an excellent fit to the data, several papers have presented evidence for potential deviations from isotropy. If real, these deviations would challenge the basic concepts of modern cosmology and dark energy. A full sky BAO survey not only produces a measure of $H(z)$ averaged across the sky, but that measurement can be examined for isotropy, assuming nearly full sky coverage (Clarkson, Bassett, & Lu 2008). If the reported deviations from statistical isotropy are real, then this might become the most important measurement made by JDEM.

Integrated Sachs Wolfe (ISW) Effect

A combined analysis of full-sky CMB maps together with the nearly full sky JDEM galaxy redshift survey provides a measurement of the Integrated Sachs Wolfe (ISW) effect of gravitational redshifting since the surface of last scattering. This late-time ISW effect is particularly sensitive to dark energy, and constitutes an additional JDEM test of the nature of dark energy (Hu & Scranton 2004).

Long Wavelength (2 - 4 micron) Survey

A unique and valuable measurement of the growth of structure in the Universe can be made with a survey of ~1000 square degrees in the 2-4 μm band. The benefits of such a survey are discussed in Appendix C. Although the SCG concluded that such a survey would be valuable for DE studies, the Project Office was not able to fit the long

wavelength (cold telescope) capability on the RM in addition to the instrumentation for the other 3 techniques.

Galaxy Clusters

Clusters of galaxies are the most massive objects in the Universe to have undergone gravitational collapse. The abundance of the most massive clusters in redshift space is a sensitive test of Dark Energy effects. Galaxy cluster surveys have to date been done either by optical identification of clumps of red cluster member galaxies, or by x-ray detection of the hot intracluster gas. Millimeter-wave searches for galaxy clusters via the Sunyaev-Zeldovich (SZ) effect are underway. All three methods can discover many thousands of galaxy clusters, and the accuracy of dark-energy constraints will likely be limited by the accuracy with which these galaxy counts, x-ray, or SZ signals can be related to the dark-matter content of the clusters.

JDEM can significantly enhance the power of cluster cosmology in several ways. First, the optical identification of clusters, and the assignment of redshifts to x-ray or SZ-selected clusters, all depend upon photometric redshift and typing of cluster members. For clusters at $z \geq 1$, near-infrared photometry is necessary for reliable cluster photo-z's. JDEM is uniquely capable of deep wide-field NIR surveying. JDEM is also uniquely capable of a deep weak lensing survey that can detect and characterize galaxy clusters by their gravitational lensing signatures. WL detection responds directly to dark matter content, bypassing the principle systematic error of other methods.

For JDEM to make a strong contribution to galaxy-cluster dark-energy constraints, it is critical that the JDEM survey strategy be contiguous on the few-arcminute scale of galaxy clusters. Controlled selection and measurement of clusters would be extremely difficult if most clusters in the survey had substantial swaths of missing data across them. This is strong incentive for JDEM to implement a filled-sky survey.

Redshift-Space Distortions

The growth of structure due to gravity causes peculiar velocities with respect to the smooth Hubble flow. Since these features depend on the growth of structure, which in turn depends on gravity, observations of redshift-space distortions can be a powerful probe of modified gravity models. The line-of-sight is a preferred direction when redshift is used to measure distance. Systematic differences in the distribution of galaxies in real space versus redshift space provides information related to both the background cosmology and the bias of galaxies (Kaiser 1987). JDEM's large spectroscopic redshift survey for BAO will provide unique data for a sensitive measure of redshift-space distortions.

IV. JDEM Scientific Requirements

Appendix A gives the full JDEM requirements developed from inputs by the SCG

subgroups for the BAO, SN, and WL methods. Listed below are a few key criteria that were scaled to fit the three techniques into the current Reference Mission and still achieve the capability for order-of-magnitude, space-unique improvements in dark energy measurements.

There are supporting ground-based observations that are needed to meet the JDEM science goals. The two key requirements in this area are blue/UV galaxy photometry over >10,000 square degrees, plus light curves and spectra of supernovae at z<0.2. The ground observations must meet the JDEM specifications for data quality---in particular, photometry that is reliably tied to the JDEM system with <0.01 mag error.

Table 1: BAO RM Criteria

Parameter	Criterion
Bandpass	1.1 - 2 microns (spectroscopy) NIR (imaging)
Survey Depth	H_{AB}> 23.5 at 7σ imaging <1.6 x 10^{-16} ergs /cm^2-s 6.5σ spectroscopy [1]
Effective Area (sky coverage x $nP/(1+nP)^2$ at z=2)	7500 sq deg
Survey Sky Coverage [2]	≥ 20,000 sq deg
Density of Galaxies Detected [2]	>4.5x10^{-4} per Mpc^3 (1.8 x min zodiacal bckgnd)
Number of Galaxies Detected [2]	≥ 1.4 x 10^8
Dispersion Resolution [3]	200-240 arcseconds
Spectroscopy [4]	4 spectroscopic views with opposed dispersions
Redshift measurement accuracy (1σ)	0.001 (1+z)
Pixel Scale	≤ 0.5 arcseconds per pixel

[1] Galaxy with an exponential profile of 0.35 arcseconds halflight, z=2, 1.8 x min zodical light background

[2] Effective Area is key requirement. These 3 rows are an example of a possible implementation.

[3] From "BAO Resolution Report link on public JDEM SCG web site (http://jdem.gsfc.nasa.gov/scg.html)): We require a dispersion in the range

200 arcseconds $\leq \lambda(d\Theta/d\lambda) \leq$ 240 arcseconds.

The requirement applies everywhere over the full focal array. It specifies the product $\lambda(d\Theta/d\lambda)$, where λ is the observed wavelength in Angstroms, and $d\Theta/d\lambda$ is the dispersion in

arcseconds per Angstrom. The dispersion requirement derives from the BAO redshift accuracy requirement

$$\sigma_z / (1+z) = \sigma_\lambda/\lambda \leq 0.001$$

which can be recast in terms of the angular centroid uncertainty and the dispersion

$$\sigma_\Theta / \lambda(d\Theta/d\lambda) \leq 0.001.$$

Here σ_Θ is the 1-σ uncertainty in angular centroid of the line, which has statistical and systematic contributions. The dispersion requirement is not independent of the centroid accuracy requirement.

[4] Spectroscopic confusion is a concern. Small rolls (~2 deg) are a possible way to reduce confusion.

Table 2: SN RM Criteria

Parameter	Criterion
Bandpass	0.38 - 2 microns [1]
Redshift Range	$0.3 \leq z \leq 1.2$ [2]
Number of SN per Δz=0.1 bin	>200
Total Number of SNe [3]	>1800
Spectroscopic Resolution	R = 75 per 2 pixels (slitless)
Telescope Minimum Diameter	1.5 m
SN Sampling Cadence	≤ 5 days
Survey Area x Time at z>1	10 sq deg years
Photometric Bands (filter wheel)	10 filters + grism / prism
Pixel Scale	< 0.27

[1] Throughput in 0.38 - 0.5 micron range can be reduced by factor of ~3 due to intrinsic brightness of nearby sources

[2] The redshift range (and numbers of SNe) depends on the actual SN rates. Taking the 1-σ lower error bar of the Dahlen et al (2008) rates would reduce this redshift range, or require consideration of Reference Missions with somewhat larger A Ω $t_{mission}$.

[3] Total number of SNe derived from redshift range and number per redshift bin requirements.

Table 3: WL RM Criteria

Parameter	Criterion
Photo-z Bandpass	0.38 - 1.7 microns[1]
Shape Measurement Bandpass	0.5 - 1 microns

Survey Sky Coverage [2]	$\geq$ 10,000 sq deg
Sky Density of Galaxies Detector (n_{eff}) [2]	$\geq$ 30 per sq arcminute
Number of Galaxies Detected [2]	$\geq 1 \times 10^9$
Pixel Scale for Shape Measurement	$\leq$ 0.2 arcseconds per pixel
Photo-z Number of Filters NIR	3
Photo-z Number of Filters Visible	5 [3]
PZCS wavelength range	0.5 - 1.7
PZCS emission line flux threshold	1×10^{-17} erg/cm^2-s (5σ)
PZCS survey area	$\geq$ 1 sq deg

[1] Full photo-z bandpass. The RM assumes 0.5 - 1.7 microns will be done on board. 0.38 - 0.5 on ground
[2] Survey sky coverage, sky density of galaxies and number of galaxies requirements are not independent but must meet combined requirement of all three.
[3] RM assumes 3 filters on JDEM and 2 filters on ground

V. JDEM Design Notes

The following are notes on the JDEM design based on discussions of the SCG.

1) JDEM benefits by enabling all 3 primary techniques for dark energy study: SNe, WL and BAO. Each has unique potential for progress on understanding the nature of DE. Combining the 3 provides enhanced figures of merit for dark energy parameters and gives cross-checks between the methods.

2) JDEM's purpose is to provide dark energy measurements which can be uniquely or best done from space. Space capabilities that enable dark energy progress include wide-field infrared photometry and spectroscopy, good seeing and low sky background above the NIR-bright, scintillating atmosphere, excellent systematics error control in the stable environment of L2, and round-the-clock full-sky survey measurement capability using well-characterized and unchanging instrumentation.

3) BAO is a powerful new technique for dark energy study based on a large-scale spectroscopic NIR survey of emission-line galaxies. The BAO signal is measured to to within a factor of two of the cosmic variance limit in the $0.7<z<2$ range available from space. JDEM will provide redshifts and positions of 2×10^8 emission-line galaxies in the 1.1-2 micron band. This BAO 3-D survey will provide a robust measurement of $D_A(z)$ and the valuable direct H(z) that depends only on the geometry of galaxy separations. A prism with resolution $\lambda\, d\Theta/d\lambda = 200$ is needed for slitless spectroscopy to give the required accuracy for the galaxy redshift measurement and to allow the OIII split line to be resolved and distinguished from Hα. BAO puts only modest requirements on observatory pointing and stability capabilities, but requires a JDEM optical configuration that enables wide-field spectroscopy over a broad wavelength range.

4) SNe is a well developed technique, currently providing strong constraints on dark energy based on a direct luminosity measurement of $D_L(z)$. JDEM will provide lightcurves and spectra of >1000 SNe Ia extending into the space unique redshift range of z>0.9. In addition, observations of SNe in the restframe NIR can provide lower dispersion in the peak magnitude determination than at shorter wavelengths. The stability of the spectrophotometric calibration also improves the accuracy of the Hubble diagram well beyond what is available from the ground at all redshifts beyond z>0.25.. SN observations put moderate requirements on spacecraft pointing and stability and strict requirements on photometric knowledge. Spectroscopy (dispersive or slit) is required for redshift and SN type measurements. If spectra are obtained with the high signal-to-noise available in space, they can further improve the statistical/systematic accuracy of the Hubble diagram.

5) WL is a powerful new technique for dark energy study based on an imaging survey of galaxies in the $0 < z < 4$ range. JDEM will provide high-accuracy shape measurement of galaxies to detect the coherent ellipticity caused by gravitational lensing. Observations with a stable, well-characterized optical train above the atmosphere provide reliability on shape measurement that cannot be obtained from the ground. Space-unique NIR filters combined with visible filters on board and on the ground give photometric redshift determinations for each galaxy. Space-unique deep NIR spectroscopy, combined with ground-based spectroscopy, provide a highly complete redshift survey to calibrate the photometric redshift system. Galaxy shapes and redshifts of 1-2 x 10^9 galaxies will provide a precise measurement of the growth of gravitational fluctuations over cosmic history. WL benefits from the wide field and high angular resolution available with space-based telescopes, and requires a stable observatory with precise knowledge of its pointing and optical fluctuations.

6) JDEM will exploit the opportunity uniquely offered by a space observatory to:
- push SN observations into NIR to z>1 with good statistics & systematics
-measure SNe at z<1 in the rest-NIR and with highly stable calibrations to improve precision and accuracy of the Hubble diagram
- perform a large sky-area BAO survey in the NIR to within a factor of two of the cosmic variance limit
- provide a BAO measurement with the large cosmic volume to z=2
- perform a large sky-area WL survey with low shape-measurement systematic errors
- provide deep NIR imaging for photometric redshifts of the galaxies in the WL, BAO, and SN fields.

7) A reference observing program has 4.4 years dedicated to sky surveys for WL and BAO giving 10,000 to 20,000 sq degree coverage, respectively, plus 2-3.5 years (survey time depending on actual SN rate) dedicated to SNe monitoring of a few sq degree high-latitude field giving 750-1500 SN Ia detections. This will yield dark energy measurements with an order of magnitude improvement in DETF FoM if supplemented with ground data to provide precision photometry in visible filters for the WL photo-z measurements and for lightcurves of low redshift SNe. The Reference Mission is capable

of obtaining these data, but would require additional observing time. It is expected to be less expensive to obtain these data from careful ground-based observations.

VI. Description of Reference Mission

The JDEM Project Office was tasked with defining a Reference Mission to be described in the NASA Announcement of Opportunity for dark energy scientific investigations. The purpose is to have a common mission configuration to which responders can propose. In addition, this Reference Mission is to be used as the starting point for Phase A optimization studies. The Project Office developed several RM concepts based on the requirements developed by the SCG. These concepts were evaluated against the science requirements by the SCG and iterated upon to reach the current RM design.

Many key design constraints were considered in producing the RM. An important one was keeping the scope and complexity low. Maintaining low risk and selecting configurations with high Technology Readiness Level (TRL) components were also significant considerations. Another key objective was to meet the requirements as best as possible for all three of the Dark Energy investigation techniques previously identified. This section describes the RM and the following section discusses its performance capabilities.

Enveloping requirements

The Project Office chose an afocal optics design for optimum performance and ease of accommodation of the BAO prism.

BAO requires a large field of view to observe at least 20,000 sq. deg, with a goal of 28,000 sq. deg, all sky minus ecliptic and galactic planes, in an acceptable amount of time. With limits on detector device or pixel count, pixel scales tend toward 0.5 arcseconds per pixel for BAO-optimized systems.

SNe require large aperture area times throughput for deep imaging and spectroscopy needed to identify, classify, and determine the redshift of sufficient numbers of Type Ia SNe in an acceptable amount of time.

WL requires large sky coverage, ~10,000 sq. deg, but with much finer sky sampling than BAO and even SNe to resolve galaxy shapes. With fine dithers included in the WL observations, a maximum plate scale of 0.20 arcseconds per pixel was specified.

The RM solution chosen by the Project Office for this set of requirements is a relatively large aperture telescope with multiple focal lengths and an afocal space.

The thermal stability, stray light and large sky coverage requirements of the mission resulted in an Earth-Sun L2 libration point orbit being selected for the RM. The field of regard for the mission is any point between 80° and 120° off the Sun. A mission life of 5

years was a specified design constraint, and a goal has been established that consumables should allow at least a 5 year mission extension.

The RM design focused on the instruments and telescope, also called the payload. The payload and spacecraft together make up the Observatory. The reference mission Observatory design is shown in Figure 4. The Observatory is ~9 m long and ~ 2000 kg. Each of the elements of the Observatory is described below.

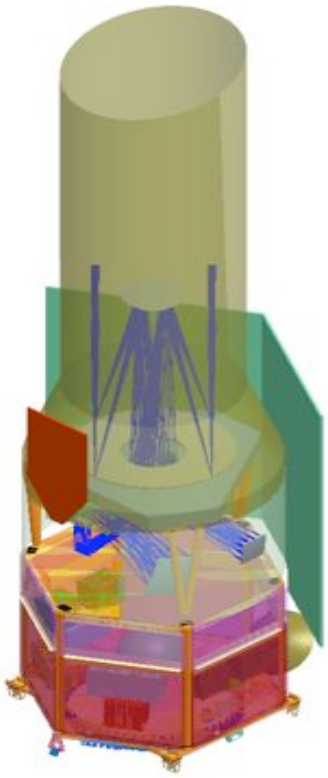

Figure 4 Observatory configuration

In its consideration of the other RM designs the SCG noted a few directions that may provide flexibility for the Phase A design studies.

1. Use of prisms in a converging beam to achieve the high dispersion values used in the BAO measurements.
2. A combination of the NIR imager and spectrometer into a single NIR channel with a common pixel scale.
3. A focal design for all channels

Telescope

All telescope designs studied were three mirror anastigmats (TMAs). These designs offer the widest field of view along with a flat focal plane and good correction of low order aberrations such as coma, spherical aberration, and astigmatism.

The current design uses an afocal TMA working at a pupil demagnification of 15 (100 mm pupil diameter). A 1.5 meter diameter primary mirror feeds three separate tertiary mirrors for an imaging arm and two copies of a spectroscopic arm. The imagers include a dichroic at ~0.98 μm splitting the input light to separate CCD and HgCdTe focal planes. The total field of view is ~1 square degree.

In order to separate the beams from the different channels, the TMA is corrected at a large radial field half angle of 1 degree; therefore, the extremes of the different fields of view are separated by up to ~2.5 degree. This implies a rather large radius for the primary mirror (PM) stray light baffle with some vignetting expected to be required to control stray light, along with a significant secondary baffle.

The optical telescope assembly (OTA) reflecting surfaces are required to be <243K to limit the in-band thermal emissions to ≤10% of the minimum zodiacal background.

The tertiary mirrors and associated fold mirrors, including the imaging channel dichroic, are all included in the OTA, so that the interface to each instrument channel is a collimated beam and each interface can be tested by a combination of collimation tests and pupil alignment tests. The secondary mirror has a 6 degree of freedom mechanism to adjust the focus and alignment of the secondary mirror.

Instruments

In the RM design, the all-reflective Visible (VIS) imager uses the same tertiary mirror as the NIR imager via a dichroic. The optical interface to the telescope is at the afocal pupil, but no pupil mask is needed for the CCD imager. The VIS imager optical path consists of an 8-position filter wheel, a shutter, two powered mirrors, a fold mirror, a field lens, and the CCD focal plane. It works at an f/ratio of f/7.4 to produce a pixel scale of 0.20 arcseconds per pixel with 10.5μm pixel CCD devices in a 3x3 layout covering approximately 0.6 degree by 0.6 degree for a total of 0.36 square degrees. Notionally, the CCD focal plane can be operated at ~180K.

The near IR (NIR) imager is a refractive camera, consisting of a cold pupil mask, 8-position filter wheel, 3 lenses and a thin corrector lens just in front of the HgCdTe focal plane. It works at an f/ratio of f/9.9 to produce a pixel scale of 0.25 arcseconds per pixel with 18μm pixel HgCdTe devices with a 2.5 μm cutoff in a 2x4 layout covering approximately 0.6 degree by 0.3 degree for a total of 0.18 square degrees; however, a bandpass filter will cut off the red end wavelength at 2.0 μm. The instrument and detectors will be passively cooled to enable zodiacal background limited sensitivity, with

~140K-170K (instrument) and ~75K-100K (detector) being representative operational temp ranges. The NIR imager is half the field of view of the VIS imager.

Both imagers will include slitless R~75 dispersive elements in the filter wheels for spectroscopy.

The NIR spectrometers are also refractive, consisting of a fixed prism pair, three lenses each and a thin corrector lens just in front of each of the HgCdTe focal planes. The fixed prisms are arranged to disperse 180º apart on the sky to reduce source confusion without the need to revisit the field at least 5 months later in the mission. It works at an f/ratio of ~f/5 to produce a pixel scale of 0.50 arcseconds per pixel with 18µm pixel HgCdTe devices with a 2.5 µm cutoff in a 2x2 layout covering approximately 0.6 degree by 0.6 degree for a total of 0.36 square degrees for each spectrometer arm; however, a bandpass filter will cutoff the red end wavelength at 2.0 µm, just like the NIR imager. The spectrometers will be operated at the same temperature as the NIR imager.

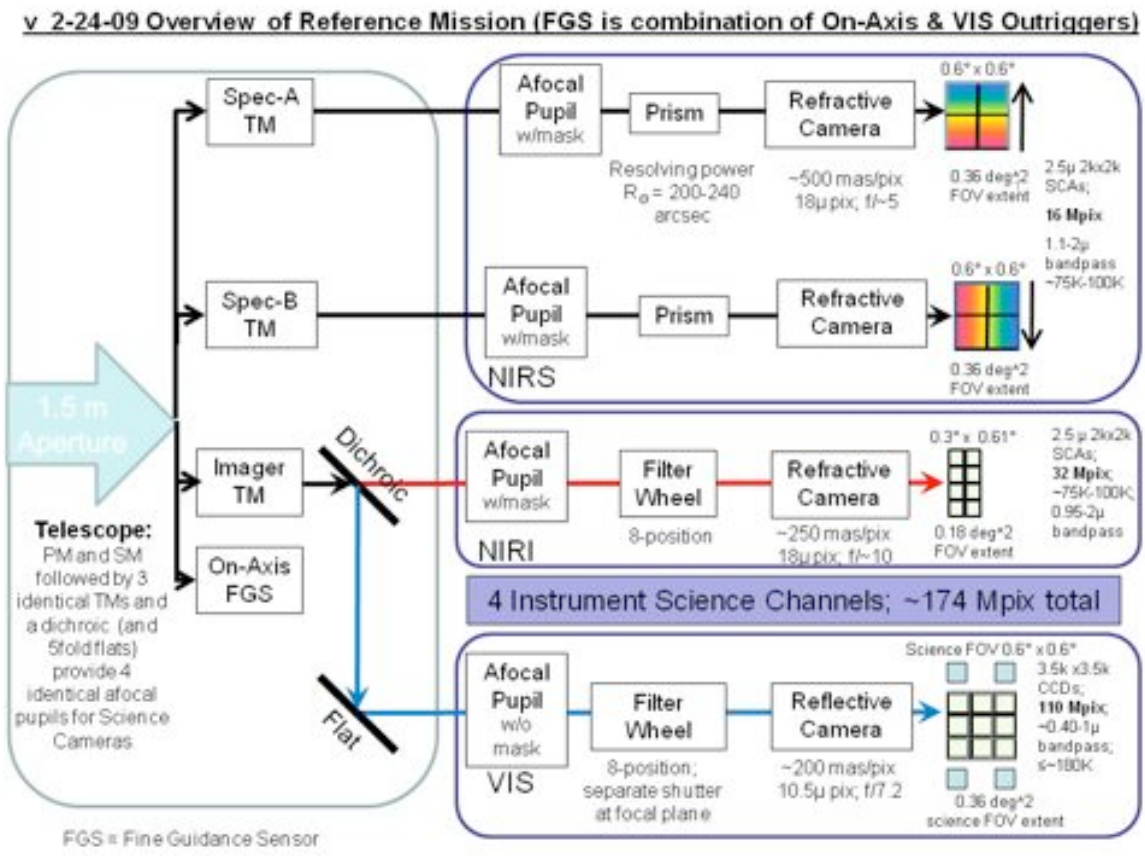

Figure 5 – RM Payload Block Diagram

Fine Guidance Sensor

The fine guidance sensor (FGS) will be used to meet the fine pointing requirements needed for the WL and SNe techniques. The primary FGS consists of 2 pairs of CCD or HyViSi detectors, a prime and redundant, located on unshuttered outriggers on the VIS imager focal plane and fed through the VIS imager optical train, including the VIS filter wheel. This guider is used in all observations that include visible imaging. An additional pair of detectors will be fed from a separate field on the telescope axis by a separate optical train which is both unfiltered and unshuttered. The on-axis guider provides pointing ability to the level required for visible or NIR spectroscopy, as well as provides adequate pointing control, in combination with Star Tracker inputs, for BAO and SN spectroscopy in the event that a filter wheel failure disables the Vis imager FGS sensors.

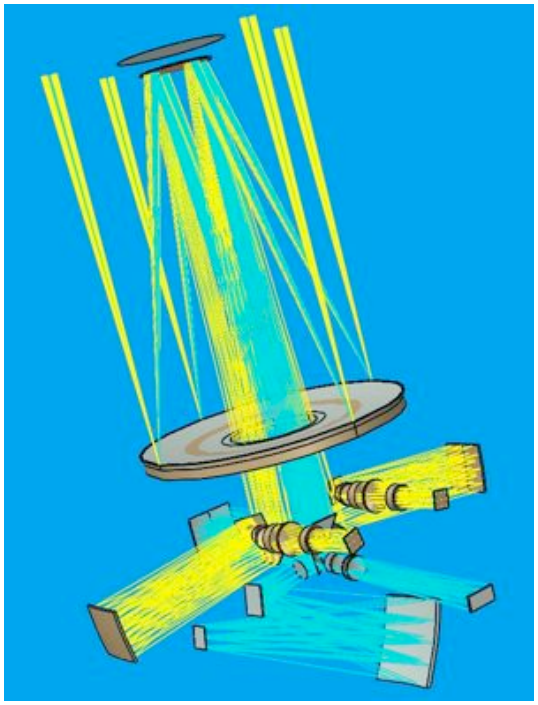

Figure 6 – RM Optical Layout

Spacecraft

The spacecraft provides the required structural, thermal, electrical, attitude control, propulsion and data/communication systems needed to support the instruments over the life of the mission. The spacecraft design for JDEM is based on the Solar Dynamics Observatory (SDO) spacecraft designed at GSFC. The spacecraft bus is a hexagonal structure housing the spacecraft electronics boxes, payload electronics boxes and propulsion tank. The spacecraft is 3-axis stabilized and uses data from the FGS to meet

the fine pointing requirements and pointing knowledge requirements of the instruments. A propulsion subsystem is required for orbit insertion and maintenance, dumping momentum from the reaction wheels and for repositioning the observatory at the end of mission life. On-station thruster activity will be managed to coincide with large attitude maneuvers, so as to avoid impact on observing efficiency. The power subsystem has a fixed solar array, sized to provide adequate power at the end of mission life with the sun at a roll angle of 45° relative to the axis of the telescope. The communications subsystem uses S-band transponders to receive commands from and to send real-time housekeeping telemetry to the ground, in addition to their use for ranging. A Ka-band transmitter with a gimbaled antenna will downlink stored science and housekeeping data at a downlink rate of ~150 Mbps to the ground on a daily basis. The command and data handling subsystem includes a solid state recorder (SSR) of sufficient size to store two full days of science and housekeeping data, in case a ground contact is missed.

Ground System

The JDEM Mission Operations Ground System (GS) is comprised of three main elements: the facilities used for space-ground communications and orbit determination, science & mission operations centers and facilities for science data processing, data archiving and science community support. The NASA Deep Space Network (DSN) is used for spacecraft tracking and provides data and command paths. The DSN receives the downlinked data from the observatory and forwards it to the mission operations center. Commands generated by the operations centers are also uplinked to the observatory via a DSN station. The mission operations center performs real-time functions such as telemetry decommutation, limit checking, telemetry display, commanding and Level 0 & 1 processing of the science and engineering data. The data processing and science centers perform Level 2 & 3 science data processing and support the science teams and the general astrophysics community by providing tools to analyze the data as well as by developing software to implement new algorithms. They also prepare the mission observing schedule. The data archive accepts all Level 0-3 (and higher) science and engineering data and stores it indefinitely. It provides data search and access tools to the science community and supports efficient delivery of archival data to the user community.

Calibration:

Calibration is crucial to JDEM's success. Although knowledge of the JDEM focal plane array behavior is important, what is absolutely critical is knowledge of the change in behavior. Each of the dark energy methods has one or more Level 1 and Level 2 requirements that demand very high precision calibration:

a) Photometry. SNe require ~0.5% relative uncertainty in the filter zeropoints in order to meet the requirement of 0.5% tilt over an octave in wavelength, while the photometric redshifts for WL need accuracy of ~1%. Key is photometric system stability to better than 1% .

b) Shape. One of weak lensing's most challenging systematics is the uncertainty in the measured shape of galaxies. In turn, this demands high precision knowledge of

geometrical distortion (e.g. PSF, CTE), etc. as well as constraints on the spacecraft (e.g. jitter, pointing). WL places the strongest constraints on geometrical stability of the imaging channels.

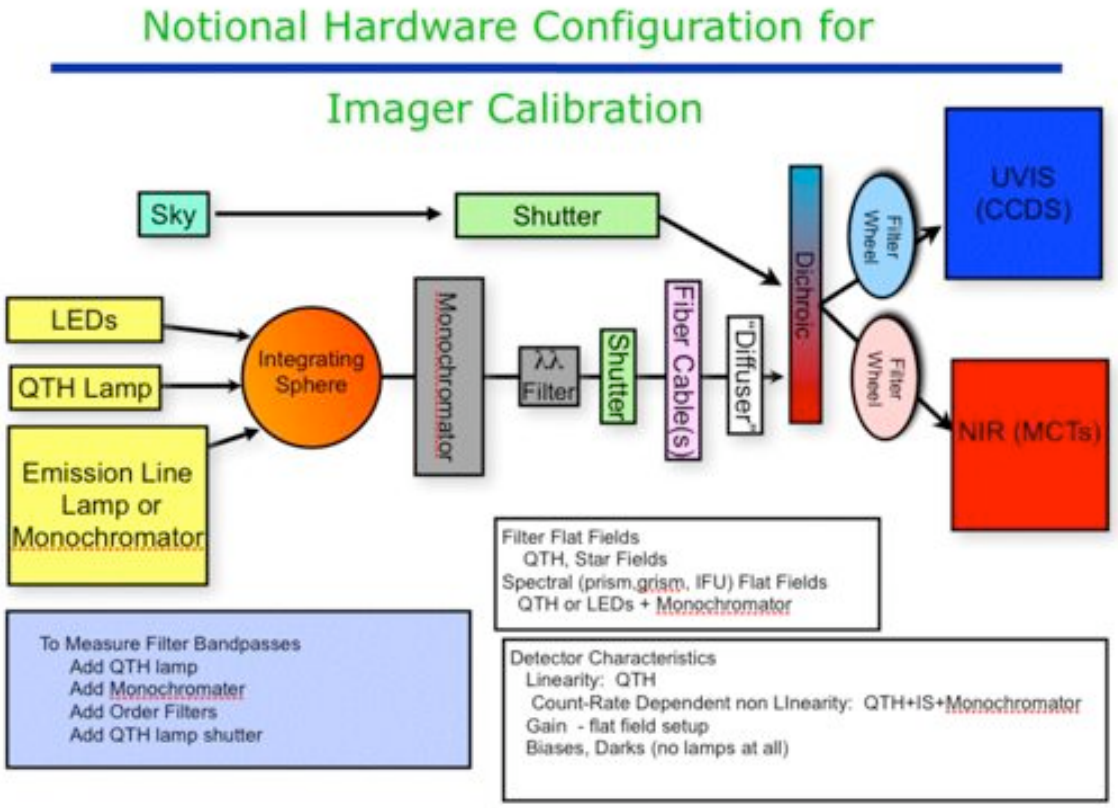

In addition to operational calibration activities which will impact the observing schedule of JDEM, these demands also naturally lead to an on-board calibration subsystem primarily needed for SN photometry. The hardware for which will include

a) An internal flat field system to generate monochromatic flat fields required for prism/grism solutions, as well as for checking/verifying filter and detector properties. Components are lamps (LEDs, QTH), a monochromator, an integrating sphere, wavelength selector, fibers or light pipes.
b) A diffuser providing smooth illumination of the focal plane arrays. This will likely be a separate part, or perhaps a spectralon sheet on the back of an existing shutter.
c) At least one shutter for the light source
d) Monitor photodiodes (InGaAs, Si)
e) Associated electronics

In an ideal case, the photometric calibration benefits from having a separate spectroscope (perhaps an IFU) to transfer calibration from the bright, standard stars to the much fainter science targets.

Because calibration is so crucial to JDEM's success, we recommend a complete end-to-end test of the assembled telescope + instruments response over the wavelengths of interest (i.e. from photon to first mirror, through the optics, to detectors), in thermal vacuum, prior to launch to characterize the ground truth. This external system will need to project monochromatic, calibrated, irradiance flat field and/or point sources into telescope front end.

Integral Field Unit (IFU)

The RM does not include a slit spectrometer but there are features of such an instrument that make it attractive for possible inclusion in the mission at a later date. In particular, an IFU (reference) was studied by the SCG and found to be powerful for SN spectroscopy. It uses a mirror with multiple facets to deflect light from individual sources to a prism spectrometer. It provides R=75--100 visible-to-infrared spectrophotometry with 100% fill factor for every pixel in a 3 arcsecond by 6 arcsecond field of view at a pixel scale of 0.15 arcseconds per pixel. A more detailed description of the IFU and its benefits for the overall JDEM mission (including SN spectroscopy and photometric calibration) are given in Appendix B.

VII. Reference Mission Capabilities

RM Design Features:

The RM has several design features important for its scientific performance as follows:

1) Large primary mirror (1.5 m diameter) and instrument fields of view (0.64 square degree NIR spectrometers, 0.16 square degree NIR imager, 0.32 square degree visible imager). $A\Omega$ is 11,000 cm^2 square degrees for the NIR spectrometers, 2800 cm^2 square degrees for the NIR imager and 5700 cm^2 square degrees for the visible imager. The total sky coverage of the NIR spectrometers and visible imager is an impressive ~1 square degree.

2) Optimized pixel scale provided by magnification in telescope design. This allows appropriately large pixel scale for the NIR spectrometer (0.5 arcseconds per pixel) for maximum sky coverage, moderate pixel scale for the NIR imager (0.25 arcseconds per pixel) for adequate PSF sampling and sky coverage and small pixel scale for the visible imager (0.2 arcseconds per pixel) for WL shape measurements

3) Dual NIR and visible imagers to give SN lightcurves and WL photo-z redshift over a wide range of wavelengths.

4) NIR imaging for the BAO galaxies to complement the NIR spectroscopy with a resolution of 200 arcseconds $\leq \lambda(d\Theta/d\lambda) \leq$ 240 arcseconds.

5) Filter wheels on the imager for maximum flexibility in choosing observing strategy on orbit. Adequate filter slots for SN and WL requirements.

6) WL shape measurements primarily with stable CCD detectors. Some shape information additionally available from HgCdTe detectors in the NIR imager.

7) Dual NIR spectrometers with fixed prisms of opposite dispersion for spectral measurements with low systematic errors.

8) Relative field of view sizes for spectrometers and imagers appropriate for BAO and WL. The optimum ratio of fields of view is 4:1 for BAO for the NIR spectrometer and imager and 2:1 for WL for the visible shape measurements plus photo-z's and NIR photo-z's.

9) High heritage HgCdTe sensor chip assemblies and focal planes with free sides for easy harness access and dense packing.

RM Capabilities

The RM has the following capabilities:

1) WL sky coverage of 3100 square degree per real year, assuming a 75% observing efficiency.

2) BAO sky coverage of 8440 square degree per real year, assuming a 75% observing efficiency

3) SN sky coverage of ≈5 square degree every 5 days, assuming a 75% observing efficiency. This gives 375-750 SN detections per year in the redshift range $0.3 < z < 1.2$, depending upon the astrophysical rates and details of the survey strategy.

4) Fixed prisms with resolution $\lambda\, d\Theta/d\lambda = 200$ arcsec for BAO. Filter wheels with ~5 filter each for the NIR and visible imager plus a grism or prism with a resolution of 75 for SNe.

VIII. Reference Observing Strategy

There are many different combinations of WL, BAO and SN observations that can be done with the RM. The observing strategy can, in fact, be optimized while on orbit based on early results from the mission. We lay out below a strategy with 4.4 years devoted to combinations of WL and BAO sky surveys and 2 years devoted to SN observations. In practice observations from the different techniques could be interspersed with each other with, for example, SN observations done for a few hours every day. The figures of merit

for these notional observing plans are evaluated as a function of SN observing time in the next section.

1) Joint WL/BAO survey. 3.2 years duration. Sky coverage of ~10,000 square degrees.

2) BAO dedicated survey. 1.2 year duration. Sky coverage of ~10,000 square degrees (in addition to 10,000 square degrees of WL/BAO survey to give a total BAO coverage of 20,000 square degrees).

3) SN monitoring. 2-3.5 years total duration depending on actual SN rates (possible to intersperse with WL and BAO surveys). 375-750 SNe observed per year, including time interspersed with WL and BAO.

IX. Figures of Merit for Reference Mission

We evaluate the ability of the Reference Mission with Reference Observing Strategy to constrain dark energy and test general relativity using the prescriptions of the Figure of Merit Science Working Group (Albrecht et al. 2009). The FoMSWG provided an estimate of the quality of data before the launch of JDEM and suggested three classes of Figures of Merit:
(1) the Dark Energy Task Force (DETF; Albrecht et al. 2006) FoM describes the (inverse) area of the expected error ellipse in the (w_0,w_a) plane;
(2) the γ FoM is the (inverse) variance in the estimate of rate of gravitational growth since z~5;
(3) the principal component (PC) FoMs give (inverse) variances of principal components of the *w(z)* function. The PC FoMs describe the ability of an experimental suite to constrain a wider variety of *w(z)* behaviors.

We adopt the FoMSWG pre-JDEM data models and assume they will be improved by JDEM observations as follows:

- **CMB**: we adopt the FoMSWG Planck data model as described in Albrecht et al (2009).
- **BAO**: The FoMSWG pre-JDEM model assumes a 10,000 deg^2 survey with ***nP=3 (TBD)*** for 0.1<z<0.7 and 400 deg^2 survey at 1.8<z<3.4. We assume that the JDEM BAO survey coverage from the RM description in Table 4 will supplement the ground data. We also presume that ground-based surveys will double the z<0.7 coverage during the JDEM era. BAO forecasts follow Seo & Eisenstein (2007). With the careful mission design, the BAO survey will be limited by statistical errors so no corrections are needed for systematic errors for BAO forecasts.
- **WL**: The FoMSWG pre-JDEM WL model assumes a survey of 5000 deg^2 with source density n_{eff}=10 arcmin^{-2}. We assume that JDEM data described in Table 4 will *replace* the ground data. WL Fisher matrices were calculated by two independent techniques: Albrecht et al (2009) and Bernstein (2008). The WL forecasts make use of shear-shear, shear-density, and density-density 2-point statistics in the imaging survey but no higher-order statistics. The correlations with

the BAO redshift-survey targets are also used, and an unbiased redshift survey of 10^5 source galaxies is assumed available to calibrate the photo-z error distribution. Systematic errors included are: redshift-dependent shear calibration errors; scale- and redshift-dependent bias and stochasticity of galaxies with respect to dark matter; scale-and redshift-dependent bias and stochasticity of galaxy intrinsic alignments with respect to dark matter; uncertainties in the baryonic contribution to the power spectrum at small scales; and errors in the photo-z error distribution, as constrained by the spectroscopic survey. The forecasted γ FoM is seen to depend substantially on non-Gaussian contributions to the power spectrum covariance due to the presence of individual massive low-z clusters in the survey. We have presented a range of potential outcomes depending on whether this additional covariance can be removed by identifying these clusters.

- **SN**: The FoMSWG pre-JDEM SN model assumes a systematics-limited Hubble diagram with independent 2% distance uncertainties in each bin of width Δz=0.1 for 0.1<z<0.5 and 3% in distance for 0.5<z<0.9, with a smaller HST-based statistics-limited sample for 0.9<z<1.6. We assume that these data will be *replaced* by the following data: ground visible/NIR data will determine distances to 0.65% in 2 bins at z<0.2. At z>0.2 we forecast the number of SNe for which JDEM can obtain full light curve photometry and spectroscopic redshifts from slitless spectroscopy during 2 years' use of the Reference hardware. In an optimistic scenario, SN event rates are high enough (Dahlen et al 2008) to reduce random errors to 0.65% in distance per Δz=0.1 bin, while lower rates give 1% errors per bin. The optimistic scenario has the spectra sufficient to use SNe to z=1.2, and we limit z<0.9 in the conservative scenario. No additional allowance is made for calibration or evolution systematics in the JDEM SN data.

Table 4: Assumed data for JDEM Reference Observing Strategy and Mission.

Method	Survey Size	Survey Depth
BAO	20,000 deg^2	0.7<z<2.0, uniform exposure time, nP=3 at z=2 for zodiacal light 1.7x ecliptic pole.
WL	10,000 deg^2	n_{eff}=30 arcmin^{-2}, z_{med}=1.1, photo-z RMS 0.04(1+z), 10^5 unbiased spectroscopic calibration redshifts
SN	1500 SNe (optimistic) 750 SNe (conservative) + ground-based z<0.2 sample	z<1.2 (optimistic) z<0.9 (conservative)

Table 5 gives the FoMs forecast for the pre-JDEM era and after completion of the 6.4-year RM. The DETF FoM is improved by 7-9x over the pre-JDEM value, depending upon the expectations for SN rates and depth. The JDEM values also represent a 15-20x

improvement over the value (≈50) that the DETF forecast after completion of "Stage II" (presently operating) projects. The improvement in the γ FoM is dramatically larger, due almost in entirety to the substantial advance in WL data quality with JDEM. The higher-order PC FoMs also improve by substantially more than 10x over pre-JDEM values.

Table 5: FoMSWG Figures of merit forecast for pre-JDEM and after completion of Reference Observing Strategy. The post-JDEM forecasts span a range dependent upon the event rate and depth of the SN survey, and the non-Gaussian statistics of clustering.

Figure of Merit	Pre-JDEM value	Value after RM
DETF (w_0-w_a dark energy)	116	800-1025
γ (growth of structure)	23	550-3000
PC (5 best-constrained modes)	2200 / 516 / 210 / 113 / 68	18,000 / 6500 / 4400 / 3000 / 2000

The strength of the FoM improvements relies on several aspects of the JDEM RM. Substantial improvement over the pre-JDEM SN accuracy, particularly the systematic-error floor, is critical to attainment of 10x improvement in DETF FoM. Augmentation of the RM with an integral field unit (IFU) for SN spectroscopy would bring this improvement into scope of a 2-year SN program even for conservative estimates of the SN event rates. The FoM forecasts are only weakly dependent on the allocation of time among the "wide-area" surveys in the Reference Observing Strategy, *e.g.* devoting the full 4.4 years of wide surveying to parallel WL+BAO observations does not significantly alter the FoMs. Similar FoMs could also be obtained with a somewhat deeper SN redshift range and somewhat smaller WL or BAO wide-area surveys.

These forecasts do not include any information to be gained from other dark energy observables. For example, reshift-space distortions will give distance and growth information if the BAO survey attains sufficiently low contamination and velocity errors. Lensing-selected or optically-selected galaxy cluster counts would give significant gains if the imaging surveys are contiguous on the few-arcminute scales relevant for cluster detection. Likewise with favorable survey geometry and performance we can expect to extract cosmological information from higher-order statistics in the WL and spectroscopic surveys. The above FoM estimates can be considered conservative in this sense.

X. Directions for Further Mission Development

Several elements of the mission design were discussed by the SCG as deserving attention during trade studies for further mission development:

1) The speed and depth of the SN program can be increased several ways: more NIR detectors, larger telescope aperture, and the inclusion of an IFU spectrometer. Relatively

small increases in these dimensions could reach the SN Requirements of Appendix A. Such design elements and possible longer SN survey times would make it possible to take full advantage of the maturity of the SN technique, with sufficient numbers of SNe and sufficiently detailed observations of each one.

2) The speed and depth of the WL program can be increased with more optical detectors and/or a larger telescope aperture. This would allow the WL program area to achieve ~20,000 sq deg (e.g., tracking the BAO program area for a symmetric FoM contribution), and/or study a larger number of galaxies per sq deg.

3) Larger numbers of both NIR and optical pixels would allow these improvements in area coverage, while at the same time improving the pixel scale.

XI. Ancillary Science

The sky surveys performed by JDEM for dark energy study will also be of great value for general astrophysics. We are entering an era of sensitive surveys across the electromagnetic spectrum and JDEM will provide an important unfilled capability, namely wide-field imaging and spectroscopy at space-enabled resolution, in the wavelength range 0.4 - 2.0 microns. The broad scientific potential of JDEM observations was highlighted in the BEPAC report and was the focus of a dedicated conference (McKay, Fruchter & Linder 2004). We briefly describe below some applications of JDEM surveys, noting that the majority can be conducted with the survey data to be obtained from the dark-energy investigations, while some would benefit from additional programs with sky coverage or cadence beyond the nominal DE observing plan.

Galaxy and matter clustering: The JDEM surveys will cover an effective volume of >200 Gpc^3, more than an order of magnitude larger sample of our Universe than existing surveys, over which it will obtain 200 million spectroscopic redshifts, 1-2 billion photo-z's and a map of the gravitational potential. The power spectra will yield greatly improved measures of neutrino and matter densities or other processes affecting the inflation-era perturbation spectrum. Nonlinear matter and galaxy evolution histories can be measured from examination of higher-order correlations in these fields; the galaxy-lensing correlations will unveil the evolution in the relation between the properties of galaxies and the properties of their host dark-matter halos.

Galaxy and AGN evolution: The JDEM slitless wide survey will detect emission-line objects over half the sky and provide resolved broadband visible-NIR images of each, revealing the full history of bright star-forming galaxies and AGN. The deep JDEM surveys will conduct a blind survey to ~10^{-17} erg cm^{-2} sec^{-1} over a few square degrees, enabling an essentially complete inventory of star-formation incidents and AGN activity for galaxies at $z<3$.

Stellar populations: The space-based resolution of JDEM will enable resolved visible-NIR stellar photometry of all systems in the Local Group and many beyond. With HST and JWST, we must choose small sections of nearby galaxies to observe, but the JDEM FOV will allow us to catalog the stars of all these galaxies in their entirety.

Strong lenses: The vast majority of galaxies have Einstein radii well below 1

arcsecon, so the JDEM wide-field survey will detect far more strong lenses than can be found from ground-based surveys, and will provide visible-NIR imaging for color selection. These objects measure the mass distribution and substructure of galaxies and clusters as well as cosmological parameters.

Brown dwarfs: The JDEM deep NIR photometric survey will vastly increase the number of known low-mass stars and brown dwarfs, with NIR colors for all and NIR spectra for the brighter ones.

High-redshift AGN and galaxies: The JDEM NIR surveys will detect the Ly-α break to $z>10$ and cover sufficient area to detect the rare bright objects at these redshifts. This will be essential to finding objects suitable for detailed study with JWST.

The Outer Solar System: JDEM could discover thousands of Solar System objects too small or distant to see from the ground, including the precursor population for km-sized comet nuclei.

Variability and transiting exoplanets: JDEM will make repeated observations of several few square-degree fields to search for high redshift SNe. Those data can also be used to identify other variable objects, including eclipsing binary stars, cataclysmic variables, pulsating variables, orphan afterglows of gamma-ray bursts and variable AGN. Indeed, the photometric stability provided by JDEM could be sufficient to permit detection of transiting giant planets. The high Galactic latitude and NIR coverage of JDEM would complement ground-based transit searches.

XII. References

Albrecht A., et al. 2006, Report of the Dark Energy Task Force Report [astro-ph/0609591]

Albrecht, A., et al. 2009, FoM Science Working Group Report, Instrumentation & Methods for Astrophys, submitted (astro-ph 0901:0721)

Alcock, C. & Paczynski, B. 1979, Nature, 281, 358.

Bennett, C. L., et al., 2003, ApJ Supp, 148, 1.

Clarkson, C., Bassett, B., & Lu, T. H-C 2008, Phys Rev Lett, 101,11301

Dahlen, T., et al. 2008, ApJ, 681, 462.

Eisenstein, D., et al. 2005, ApJ, 633, 560.

Eisenstein, D., & Bennett, C. L. 2008, Phys Today, April 2008, 44.

Hu, W. & Scranton, R. 2004, Phys. Rev. 70, 123002

Komatsu, E., et al., 2009, ApJ Supp, 180, 330

Kowalski, M., et al. 2008, ApJ, 686, 749.

McKay, T.,, Fruchter, A. S. & Linder, E. 2004, New Astronomy Reviews, 49, 335

Seo, H.-J & Eisenstein, D. J. 2007, ApJ, 665, 14.

Appendix A - Detailed Requirements

The tables in this appendix were developed for each of the three DE techniques. They represent full requirements and goals developed by the SCG for each technique as a guide for future performance enhancements and optimization .

Table A1 Baryon Acoustic Oscillations (BAO)

BAO Level 1				
SPECTROSCOPY	Minimum	Requirement	Goal	Rationale
Redshift Range		$0.7 \leq z \leq 2.05$		
Wavelength Range		$1.1 \leq \lambda \leq 2.0$ _m		As derived from redshift range and Hα emission line redshift detection
Redshift Precision [2]	1.0×10^{-3} * (1+z); 68% C.L. 1.644×10^{-3} * (1+z); 90% C.L.	1.0×10^{-3} * (1+z); 68% C.L. 1.644×10^{-3} * (1+z); 90% C.L.	0.5×10^{-3} * (1+z); 68% C.L. 0.822×10^{-3} * (1+z); 90% C.L.	
Survey Fill Factor [5]	95%	98%	100%	
Survey Sky Coverage		28,000 deg^2	28,000 deg^2	
Effective Survey Area (at all redshifts)		7500 deg^2	10500 deg^2	
Redshift/Wavelength Calibration [6]		λ-precision shall be better than 2×10^{-4} ΔV precision shall be better than 60 km/s		

n*P [3]		> 1		
BAO Level 1				
SPECTROSCOPY	Minimum	Requirement	Goal	Rationale
Dispersion (λ*dΘ/dλ) [1]		200 (-0,+40) arcseconds		
Interloper Fraction		<10% per species, <20% overall	<2% per species, <10% overall	
Pixel Scale		≤ ~0.5 arcseconds		
Minimum Detectable Line Flux [7]		≤4.4e-16 erg/cm^2-s; 6.5 σ at 1.1 μm ≤3.0e-16 erg/cm^2-s; 6.5 σ at 1.3 μm ≤2.1e-16 erg/cm^2-s; 6.5 σ at 1.6 μm ≤1.6e-16 erg/cm^2-s; 6.5 σ at 2.0 μm		
IMAGING	Minimum	Requirement	Goal	Rationale
Wavelength Range	Visible or NIR	NIR		
Number of Filters		≥1 band		
Filter Bandpasses		Any		
Survey Depth		H_{AB} ≥ 23.5 at 7 σ (within spectroscopic exposure time)		
Pixel Size		≤ 0.5 arcseconds		
BAO Level 2				
SPECTROSCOPY	Minimum	Requirement	Goal	Rationale

Spectral/Spatial Confusion Mitigation [4]		≥4 exposures per field; Dual dispersions angled by 60°-180°		
Redshift Accuracy Enhancement		Dual dispersions angled by 60°-180°		

BAO Requirements Footnotes

[1] From the "Requirement" section of the "Dispersion Requirements Document v2-19-09.pdf" (https://astrophysics.gsfc.nasa.gov/scgwiki/SCG5?action=AttachFile&do=get&target=Dispersion_Requirements_Document_v2-19-09.pdf):

The dispersion requirement derives from the BAO redshift accuracy requirement

$$\sigma_z / (1+z) = \sigma_\lambda/\lambda \leq 0.001$$

which can be recast in terms of the angular centroid uncertainty and the dispersion

$$\sigma_\theta / \lambda(d\Theta/d\lambda) \leq 0.001.$$

Here σ_θ is the 1-σ uncertainty in angular centroid of the line, which has statistical and systematic contributions. In the current version of the dispersion document referenced above, this is estimated to be

$$\sigma_\theta^2 = (\Delta\Theta_{FWHM} / (S/N))^2 + \sigma_{\theta,sys}^2 \approx \mathbf{(0.94" / (S/N))^2 + (0.10")^2}$$

where (S/N) is the signal to noise ratio of the observed line emission. The statistical error depends on the observed line which, in turn, depends on the spectrometer pixel size, the dynamic spot size, and the angular size of a typical source galaxy. The systematic contributions depend on many optical performance parameters. The individual requirements on these performance parameters flow down from the requirement on σ_θ which, in turn, follows from the redshift accuracy and dispersion requirements.

While preliminary allocations of these error sources have been made, we note that higher dispersion values allow one to set more forgiving – and less expensive - specifications on many parameters without sacrificing redshift accuracy. However, too high a dispersion results in loss of signal as one begins to resolve the NII line from the

H_ line and the H_ line itself. Given these considerations, we require a dispersion in the range

200” ≤ λ(dΘ/dλ) ≤ 240”.

The requirement applies everywhere over the full focal array. It specifies the product λ (dΘ/dλ), where λ is the observed wavelength in Angstroms, and dΘ/dλ is the dispersion in arcseconds per Angstrom.

The requirement applies for the pixel scale of 0.5 arcseconds per pixel and for optics near the diffraction limit.

[2] Requirement excludes interlopers. The goal enhances redshift space distortions.

[3] n*P is the density at k=0.2 at all redshifts, where P(k=0.20 h/Mpc) = 1600 $h^{-3}Mpc^3$ = 4400 Mpc^3. If n*P >1 at z = 2 in the highest zodi regions of the sky, it will likely be met at all z for all sky positions.

[4] Must mitigate confusion. A known example of effective confusion mitigation is to take ≥ 4 exposures per field with ≥ 2 rolls of 2°–10°. In addition to providing greater efficiency, a prism (relative to a grism) also reduces confusion.

[5] Losses of coverage due to bright stars are not counted against this requirement.

[6] Distances are measured to 0.1%, so the contribution from mis-calibrated wavelengths and redshifts (d[ln dist]/dz) must be small relative to this. The redshift precision requirement encompasses random calibration errors. This requirement is for bulk dilation.

[7] Assumes zodi of 1.8 x zodi-minimum, and galaxy of exponential profile with half-light radius of 0.35 arcseconds. The shot noise from the galaxy continuum and other in-focus astronomical sources were included in the 6.5 σ requirement. The required sensitivities must be provided taking into account all other noise sources (e.g. Zodi background, scattered light, internal emissions, detector noise, etc).

Table A2 Supernova Level 1 Requirements

	Supernova Level 1	Minimum	Requirement	Goal	Rationale
1.	Redshift Range **(a), (g)**	0.3<z<1.2	0.2<z<1.5	0.1<z<1.7	Low redshift limit provides for overlap with ground observations (same restframe measurements, systematic control and S/N) for complete coverage to z=0. SNe provide stronger DE information at z≤ 1 compared to other techniques; results at z=1 requires extending to z-1.3. SNe provide better statistics and stronger constraints on systematics if zmax is increased.
2.	SN Count/Redshift Bin**(g)**	150/Δz = 0.1	220/Δz = 0.1	300/Δz = 0.1	This number of SN is required to ensure √ N reduction to the final photometric precision required even after selection of supernova. Ensure that a large enough statistical sample is obtained including lensing statistical uncertainty. .
3.	Survey Size	>=2.5 deg^2	>=2.5 deg^2	>=3.75 deg^2	Survey size required to stay above sample variance limit due to lensing magnification. (Implies >= 18 fields at each tier for the RM) **(b)**
4.	Survey Envelope (deg^2$_t$years)	4@ z=1, 12 @ z=0.5	6.5 for z=1.5 72 for z=0.2	TBD	The survey is a product of time and area, since SN occur at rate n(z) per year per sq-degree. These numbers are consistent with the goal of obtaining the required number of SN / _z =0.1. This can be interpreted as the area to be observed over a timespan with 100% duty cycle.
5.	Minimum SN Survey Time Span		T ≥ 2 years		While a large FOV may obtain the required number of SN in a short time, this minimum time is required to follow the SN over their lifetimes and obtain reference images without SN.
6.	Sampling cadence for imaging (days)	5 days	5 days	4 days	Adequate sampling of the SN rise and fall is required. Interrupting this cadence will introduce significant observational inefficiencies.
7.	SN Ia Redshifts		Required for all SN Ia		The spacecraft must furnish redshifts for all SN events
8.	Host Imaging		R = 5 at ≤1.0μ		Host galaxy morphology and SN location in host galaxies are part of the dataset needed for analysis. Bluer imaging is

	Supernova Level 1	Minimum	Requirement	Goal	Rationale
					required for maximal resolution and sensitivity to late-type features.
9.	Distance Precision per bin (%) **(g)**	1.5 $\Delta z = 0.1$	0.7% (_z = 0.1)	0.5% $\Delta z = 0.1$	Target uncertainty (systematic and statistical including calibration) in Hubble diagram. This is the basic performance needed for Stage IV SN DE probes
10.	Peak Flux Measurement Accuracy S/N **(c)**	S/N > 30	S/N > 30 In each R=5 band		This is the basic exposure requirement for SN at all redshifts to obtain the required final distance precision. Allows dust and light-curve shape corrected distance to 0.15 mag accuracy, as well as fitting Av and Rv for each SN. See footnote **(d)**.
11.	Spectroscopy, Sensitivity S/N **(e)** Identify SNe Redshift and Type	S/N > 3	S/N > 3	S/N > 3	Identifies SNe Redshift and Type.
12.	Spectroscopy, Sensitivity S/N **(e)** Measure line ratios and velocities	S/N > 7	S/N > 9	S/N > 12	Supports resolution of correlations between spectral features and absolute magnitude. This requirement only applies if the proposed approach to SNe investigation requires it.
13.	Photometric Accuracy	1.0% tilt / octave	0.5% tilt / octave		This is a limit on the allowed systematic photometric zeropoint calibration error over the complete bandpass. Photometric accuracy propagates non-trivially into SN distances due to extinction corrections.
14.	SN 1a Redshift Accuracy	0.006	0.005	0.005 **(f)**	Effective distance uncertainty due to redshift uncertainty must be less than distance uncertainty.
15.	Survey Location	20 degree diameter disk at ecliptic-poles and high Galactic latitudes, E(B-V)<0.005			Survey areas must be continuously observable over the entire duration of the SN survey. Also minimize zodiacal background and Milky Way extinction uncertainty

Footnotes for Supernova Level 1 Requirements:

(a) Provided as a range, but requirement is separate for minimum, z_{min}, and maximum, z_{max}, redshift.

(b) Assumes contiguous survey. Ongoing study to determine number of fields required if survey is independent, not contiguous. Note that for the FILTER TABLE below, additional exposure time to account for edge effects may be required (+8%).

(c) S/N required for the observation when the supernova is +/- 2.5 days from peak brightness in each band, assuming a 5-day observer-frame cadence and the bands given in the FILTER TABLE below. The S/N requirement is redshift dependent, as 1/sqrt(1+z), since the cadence is fixed in the observer frame. S/N requirement shown is for z_{min}.

(d) S/N depends on # of bands and observed wavelength range, defined below for different central wavelengths for the minimum (blue), λ_{min}, and maximum (red), λ_{max}, bands:

S/N = 30 sqrt(6/Nbands)(1.2/(1+z)) for central λ_{min} = 0.35 and λ_{max} = 0.75 in SN restframe

S/N = 35 sqrt(5/Nbands)(1.2/(1+z)) for central λ_{min} = 0.40 and λ_{max} = 0.75 in SN restframe
S/N = 45 sqrt(5/Nbands)(1.2/(1+z)) for central λ_{min} = 0.35 and λ_{max} = 0.75 in SN restframe
S/N number in requirement table above assumes 6 bands for central λ_{min} = 0.35 and λ_{max} = 0.75 in SN restframe

(e) Defined by the S/N at restframe 0.58 μm for nominal $\Delta\lambda = 10$A (not resolution of particular spectrograph) . This number is a comparison index for the measurement uncertainty of spectral feature ratio depths and velocities. Spectral features span full bandpass wavelength range (See Requirement 2.1). The total S/N can be constructed using observations at different epochs, but with loss of certain information.

(f) Goal SN1a redshift accuracy = 0.002 for 0.1<z<0.2, 0.005 for 0.2<z<1.7

(g) Values in requirements 1., 2., and 5. can be traded against each other

SUPERNOVA EXAMPLE FILTER TABLE (1)

This table presents an implementation example, not a table of requirements

Characteristic	Value	Rationale
Log spacing between filter bands, $\ln(\lambda_{n+1}/\lambda_n)$	1.16	Log distributed filter bands required to constrain K-correction uncertainty. See FILTER TABLE instantiation.
Photometry, Resolving Power $\lambda/\Delta\lambda$ (L2 b)	3.34	Broad overlapping bands reduce exposure time. Resolving power ($\lambda/\Delta\lambda \sim 6$) reconstructed from differences in bands to provide SN and Host colors.

SUPERNOVA EXAMPLE FILTER TABLE – continued

	"Layer Cake" Tier	F0	F1	F2	F3	F4	F5 (2) VIS	F5 (2) NIR	F6	F7	F8	F9	Time/ pointing (hrs)	Pointings	
														with margin	Pain rate s
Central wavelength (μm)		0.447	0.520	0.605	0.703	0.818	0.951	0.951	1.106	1.286	1.496	1.739			
Resolving Power, $\lambda/\Delta\lambda$		3.34	3.34	3.34	3.34	3.34	3.34	3.34	3.34	3.34	3.34	3.34			
Point source magnitude (AB) that corresponds to Photometric S/N Req (R1.7) (3)	z=1.50	30.19	29.38	28.84	27.17	26.44	25.87	25.87	25.43	25.33	25.44	26.01			
	z=1.15	28.82	28.33	26.73	25.94	25.21	24.91	24.91	24.78	24.89	25.45	25.81			
	z=0.85	27.67	26.52	25.28	24.76	24.25	24.13	24.13	24.24	24.80	25.14	25.30			
	z=0.59	25.66	24.48	24.00	23.46	23.32	23.38	23.38	24.00	24.34	24.49	25.26			
	z=0.37	23.45	23.12	22.43	22.29	22.35	22.94	22.94	23.28	23.43	24.12	24.61			
Exposure time for a single visit for a single field in each filter (seconds) (4)	z=1.50	61	190	449	903	2395	2856	1634	1805	2149	2662	4714	3.6	10	8
	z=1.15	61	190	449	903	1012	850	1299	1214	1475	2525	0	1.8	0	2
	z=0.85	61	190	449	491	429	564	652	672	1087	480	480	0.94	6	6
	z=0.59	61	190	219	180	201	249	347	387	110	110	110	0.31	14	14
	z=0.37	61	71	60	63	71	96	205	50	50	50	50	0.12	88	88
Total exposure time in each filter (days) (5, 6)		30	51	66	84	150	185	182	135	144	150	237			

Note 1: Table represents a point design based on the Reference Mission concept. Many different options are possible. Therefore, this represents a specific implementation that will reach the requirements with 1.5m telescope using standard assumptions for telescope/detector specifications. Any proposed set of filter bandpasses, resolutions, and noise levels must be used in simulation to see if L1 requirements are attained.

Note 2: Filter 5 is repeated on IR and Visible Filter Wheels

Note 3: For each redshift, this magnitude is the 80% -brightness of the SNIa (i.e. MB=-18.71 for h0=0.70).

Note 4: Exposure time satisfies photometric S/N requirements for the 80% SNIa.

Note 5: Total open shutter time required for single footprint total exposure (including all visits). Assumes

survey visits are spread over 5 years at a 5-day cadence (i.e. each field is visited 365 times). Does not include read-out time. Does not include mission overhead (downlink time/day, etc). Margin taken for uncertainties in rates (the lower rate of between Pain and Lauer), host-galaxy noise contribution, and photometry degradation due to 0.25 arcsec pixels. Other margins are not included, e.g. throughput margin.

Note 6: Total exposure time in each filter cannot be coadded to equal total exposure time across all filters because of simultaneous optical/NIR imaging multiplex advantage.

Note 7: Number of filters can be traded with exposure time (i.e. If filter 0 is removed, multiply total exposure time by 2. If filter 9 is removed, multiply total exposure time by 2.5).

Table A3 Supernova Level 2 Requirements

	Supernova Level 2	Minimum	Requirement	Goal	Rationale
1.	Bandpass, λ	$0.45<\lambda<1.7\mu m$ no gaps	$0.38<\lambda<2.0\mu m$ no gaps [(a)]	$0.34<\lambda<2.5\mu m$ no gaps	Observe range where the supernova emits >90% of its flux and has homogeneous brightness. Requirement corresponds to approximately U through I band in SN restframe at all redshifts (see footnote **(a)** for other options).
Filter-based Photometry 2.	Photometric Bands (filter-based photometry)	6 filters	6 filters Optical 5 filters NIR (1 in common)		FILTER TABLE (above) presents an instantiation that satisfies constraints. See footnote **(c)** for list of constraints.
3.	Spectroscopy, Resolving Power $\lambda/\Delta\lambda$		R ~ 75 per 2 pixel spectral resolving element		Resolve spectroscopic SN features. Higher resolution requires additional exposure time to meet spectroscopy S/N requirement, R1.7.
4.	Pixel Scale		< 1.5 _ PSF-FWHM		Exposure time calculated for 0.25 arcsec pixel. Larger pixel size requires more exposure time and trade study on systematics.
Slitless prism 5.	Repeat Pointing		1/5 SCA pixel		N/A if imaging
6.	Dithering		1/3 of the PSF-FWHM		Critically sample the effective PSF.
7.	Detector Symmetry	Symmetric field every 3 months in 1-2 footprints (90 degree rotation)			

Footnotes for Supernova Level 2 Requirements:

(a) Changing of min or max wavelength from requirement to minimum range affects the exposure times required for imaging (shown in FILTER and EXPOSURE TABLES for requirement only). Exposure time multiplication factors for changing λ_{min} only, λ_{max} only and both are shown below assuming consistent restframe wavelength range over all redshifts:

$0.45\mu m<\lambda<2.0\mu m$: requirement exposure time x 2.0
$0.38\mu m<\lambda<1.7\mu m$: requirement exposure time x 2.5
$0.45\mu m<\lambda<1.7\mu m$: requirement exposure time x 5.0

Note: These multiplication factors show that larger wavelength range provides better leverage for dust extinction corrections.

(b) Maximum resolving power requirement is obtained from equation, $\Delta=(\delta+1)/2/(\delta-1)$, where $\delta = \ln(\lambda_{n+1}/\lambda_n)$ and λ_n is the central wavelength of band n. Minimum resolving power must be > 3. FILTER TABLE (above) presents an instantiation that satisfies these minimum and maximum requirements.

(c) Requirements on the bandpass, log spacing between filter bands $\ln(\lambda_{i+1}/\lambda_i) <1.19$ and band resolving power, along with the CCD QE falloff at 1 micron and the use of a dichroic (assuming dichroic position = 0.94 um), constrain the possible choice of filter bands.

EXAMPLE EXPOSURE TIME TABLE

This is an example of one approach to managing observing time, comparing different instrument configurations.

EXPOSURE TIME [1]	Ref. Mission	EXP. TIME TRADE TABLE [4]		
Aperture (constant f/#)	1.5m	1.7m	1.5m	1.7m
Number of Imaging HgCdTe Detectors, and assuming CCD matching footprint	8	8	18	18
Required SN Photometry Exposure Time (days) **(2)**	855	765	445	370
Required SN Spectroscopy Exposure Time (days) **(3)**	263	160	263	159
Total Required Exposure Time for SN program (days)	1118	925	708	529

Note 1: Table represents a point design based on the Reference Mission. Other options are provided in adjacent TRADE TABLE.

Note 2: Total photometry exposure (open shutter) time required to find and build the light curves of SN. Does not include read-out time. Does not include mission overhead (downlink time/day, etc). Margin for uncertainties in rates and host-galaxy contribution to noise is included. Other margins not included, e.g throughput margin. Assumes the Reference Mission implementation: 1.5m aperture telescope, 8-detector footprints for both CCD and HgCdTe requiring 2 pointings to get 90 degree symmetry, 0.25 um HgCdTe pix.

Note 3: Total spectroscopy exposure (shutter open) time required to achieve spectroscopic measurements to specified accuracy. Assumes an IFU. Detector noise for a 2.5 um cutoff HgCdTe device. No margin for host-galaxy brightness. Includes reference observations for 20% of the SNe.

Note 4: Total exposure time (i.e. mission lifetime) can be traded with other implementation choices such as aperture size and # detectors. If the footprint goes from 8 to 18 detectors, the imaging exposure time falls to 445 days and the spectroscopic time remains constant. If the telescope aperture goes from 1.5 to 1.7 meters and the f/# is fixed, then, despite the smaller FOV, the imaging exposure time falls to 370 days and the spectroscopy time falls to 159 days.

EXAMPLE #2 EXPOSURE TIME AND MAX SURVEY AREA:

EXPOSURE TIME	Redshift	Time
Minimal Photometric Exposure Time [(1)]	z=1	3 hours
	z=0.5	1.5 hours
Implied Maximal Survey Area [(2)]	4.7 deg^2 x 3 h/T x FOV/0.12	

Note 1: Table represents a point design. Exposure time achieves S/N=30 at peak in 5 R=5 filters over 0.9-2.0 um, assuming 1.5m primary plus separate optical channel.

Note 2: Implied maximal survey area assumes area is scanned in 5 day cadence with 100% duty cycle for given exposure time and camera FOV (sq-deg).

Table A4 Weak Lensing Level 1 Requirements

	Weak Lensing Level 1	Minimum	Requirement	Goal	Rationale
1.	neff [1]	>30 per sq arcmin		(note 8)	Value for requirement is to be determined in concert with requirement 3.
2.	Ω [2]	>10,000 sq deg	>20,000 sq deg (note 8)	>20,000 (note 8)	Minimum is derived from items 1 and 3
3.	# galaxies [1]	>1.1e9	>1.5e9	>2.2e9	Exceed statistical power of expected ground-based surveys by useful margin.
4.	Photo-z RMS error [3]	<0.05(1+z)	<0.04(1+z)	<0.03(1+z)	Effective weak lensing "tomography" and reduction of intrinsic-alignment systematic.
5.	Photo-z outlier rate [3]	<3%	<2%	<1%	Reduce cosmological biases from redshift mis-identification below stat errors Combination of 5 and 6 Reduce bias from intrinsic alignments of photo-z outliers
6.	Photo-z calibration survey (PZCS) size [4]	>30,000 galaxies	>100,000	>100,000	Unbiased spectroscopic survey to calibrate photo-z scale such that photo-z systematic errors are negligible
7.	Photo-z calibration fields [5]	>3	TBD	>5	Reduce cosmic variance in PZCS TBD plan to resolution on the timescale of 9 months in Phase A.
8.	RMS Shear calibration error [6]	<0.001	<0.001	<0.0003	Reduce shear calibration systematic error below statistical errors
9.	RMS additive shear	<0.0003	<0.0003	<0.0003	Reduce spurious shear systematic error below statistical errors Requirements 4, 5, 8 and 9 cannot be validated on hardware, they need to be validated through calculation.
10.	Sparse spectroscopic redshifts [7]	> 1 per sq arcmin, 0.3<z<1.7	TBD		Cross-correlate lensing source galaxy density/shear with spectroscopic redshifts to improve statistical errors and make robust systematic-error reductions. Ensure that the BAO survey satisfies the minimum.

Footnotes for Weak Lensing Level 1 Requirements:

(1) Galaxy counts refer to effective number of galaxies with useful shape and photo-z data, after de-weighting for shape measurement noise.

(2) Sky coverage refers to area imaged in all filters.

(3) Photo-z RMS after outlier removal. Outlier has error |ln(zp/zs)|>0.3

(4) Number of unbiased spectroscopic redshifts obtained from source galaxy sample.

(5) Number of distinct fields from which spectra are drawn. Photo z calibration field numbers are still in work.

(6) "Shear" is the gravitational lensing distortion measured by the experiment. Calibration error is a multiplicative factor by which measured shear is incorrect. Spec is RMS of this error over any subset of a source redshift distribution.

(7) Sparse spectroscopic survey are redshifts collected over >80% of WL survey area. The L1 requirements for BAO redshift survey will satisfy WL requirements.

(8) The L1 goal of 2.2e9 source galaxies can be attained by any combination of increased survey area and increased source density neff (which occurs through improved EE50 and/or image noise). The choice of route to improvement is an implementation decision. However we note that the holding the image noise level fixed requires lengthier exposures at lower ecliptic latitude, which must be included in observatory time budgeting.

Table A5 Weak Lensing Level 2 Requirements

	Weak Lensing Level 2	Minimum	Requirement	Goal	Rationale
1.	Number of photo-z filters	≥8			Achieve L1 Reqs 4,5
2.	Total Filter wavelength span	0.38-1.7 micron, no gaps		0.35-1.7 micron, no gaps	Achieve L1 Reqs 4,5 for entire source redshift range. Need to resolve the need for ground based observations as part of flight mission. A footnote will be needed as well.
3.	Filter passbands	*see Filter Table*			Achieve L1 Reqs 4,5
4.	Filter width for shape measurement bands ln(λmax/λmin)	<0.3			Limit chromatic variation of PSF, as per L1 Reqs 8,9
5.	Filter width for photo-z bands ln(λmax/λmin)	TBD			TBD closure path includes a science team investigation with engineers. Expected to be closable in phase A time frame.
6.	Number of filters used for shape (1)	≥2	≥3	≥3	Test chromatic variation of PSF compliance with L1 Reqs 8,9
7.	Exposures per filter (all bands)	≥2	≥2	≥4	Provide photometry robust to cosmic rays and pixel defects
	Weak Lensing Level 2	Minimum	Requirement	Goal	Rationale

8.	EE50 radius of PSF (all bands)	<0.35"	<0.35" (TBR)	<0.25"	Photometric accuracy, avoid crowding and loss of S/N in photometry TBR resolution path – simulation of images with degraded PSFs. Expected to be done in Phase A.
9.	EE50 radius of PSF (shape bands) (2)	<0.175"	<0.15"	<0.13"	Resolve galaxy shapes to achieve L1 Req 1 while retaining L1 Reqs 8,9. 2x improvement over best ground survey.
10.	Pixel scale (all imaging bands)	<=0.4"	TBD	<0.2"	Limit systematic errors in photometry TBD to be closed in Phase A.
11.	MTF @ Nyquist frequency, shape measuring bands (3)	<0.002	<0.002@0.9 x Nyquist	<0.002@0.8 x Nyquist	Minimize aliasing for L1 Reqs 8,9
12.	Image noise level mn (noise magnitude) (4)	*see Filter Table*	see note L1-8	see note L1-8	Attain L1 requirement 1
13.	Imaged survey area	>10,000 sq deg	see note L1-8	see note L1-8	Restatement of L1 Req 2
14.	Survey fill factor (11)	>65%	>90%	>98%	Reduce power-spectrum aliasing; goal level enables study of higher-order shear moments and galaxy-cluster dark-energy method.
15.	Number of disjoint survey fields	<=4	<=3	<=2	Chris will calculate the width of the smallest survey fields - perhaps around 20 degrees. Expects to have it by the SCG meeting.
16.	PSF second-moment uncertainty (5)	<0.001(Ixx+Iyy)	<0.001(Ixx+Iyy) (TBR)	<0.0003 (Ixx+Iyy) (TBR)	Achieve L1 Reqs 8,9 TBR closure path – initial decomposition of PSF stability requirements in Phase A.
17.	Optical bench stability (6)	<0.0003(Ixx +Iyy) (TBR)	TBD	TBD	To achieve PSF-knowledge L2 req TBR, TBD – will need to collaborate on decomposition of PSF stability into a budget.
18.	Relative pointing knowledge accuracy, RMS per axis (7)	TBD	4 mas	TBD	To achieve PSF-knowledge L2 req, observatory-motion component Relative to the position at the start of an exposure. TBDs to be resolved in Phase A.
	Weak Lensing Level 2	Minimum	Requirement	Goal	Rationale

19.	Chromatic dependence of PSF second moment [8]	< (TBD) (Ixx+Iyy)			Achieve L1 Reqs 8,9 by limiting dependence of PSF on (unknown) galaxy spectrum within filter band. Determine value of TBD closure in Phase A
20.	Chromatic Centroid Shift Across Filter Band [8]	(TBD)			Determine value of TBD closure in Phase A
21.	Spectroscopic redshift accuracy [9]	<0.01(1+z)	<0.01(1+z)		
22.	Sparse survey redshift range	0.7<z<1.7	0.2<z<1.7	0<z<2	
23.	Deep emission-line survey wavelength range	0.5 - 1.7 micron	0.5 – 1.7 micron	0.5 - 2.0 micron	Detect emission lines that cannot be economically achieved from ground, increasing completeness of PZCS
24.	Deep emission-line flux threshold [10]		1e-17 ergs/cm^2/s (TBR)		Attain L1 requirement 6
25.	Deep emission-line survey total area	>1 sq deg			Attain L1 requirement 6

Footnotes for Weak Lensing Level 2 Requirements:

(1) Shape-measurement filters should preferably include at least one pair with minimal wavelength overlap, to test for chromatic PSF systematic errors.

(2) The EE50 radius applies to the recorded image. In other words, it includes not just diffraction and optical effects, but also image blurring due to spacecraft motions and detector effects such as charge diffusion and convolution with the pixel shape. Allocation of the EE50 budget to these components is an engineering decision, not a science requirement. Similarly the MTF refers to the effective PSF on the recorded image, not just the optical MTF.

(3) This constraint embodies the sampling-density requirement. If samples are taken on a grid of side length s, then the Nyquist frequency f=1/2s is the highest un-aliased spatial frequency. We require that the amplitude modulation transfer function (MTF) be below the specified level at the Nyquist frequency for s. Note that interlaced MxM sub pixel dithering grid with pixels of size p gives sampling density s=p/M.

(4) (The level of noise in the images is measured by the noise magnitude, defined as follows: all sources of noise (both photon noise and detector noise) in the delivered images are considered, and multiple exposures in a single filter are combined into a single image. When this image is binned down to 1 arcsec square pixel, calculate the RMS flux variation in background for these pixels. Convert this flux to the AB magnitude system: this is the noise magnitude. It is a measure of the white-noise level in the final data product for that filter. Each filter band has a different requirement.

(5) The size and shape of the image PSF must be known to this accuracy at locations of all galaxies in every exposure (>99% of all galaxy images recorded). The PSF size and shape are defined by the Gaussian-weighted second central moments of the PSF: size=(Ixx+Iyy); shape e1=(Ixx-Iyy)/size; shape e2=2Ixy/size. Each must be known to the required fraction of the nominal PSF size.

(6) This specifies the amount of change to PSF moments that can occur due to change in the configuration of any component of the optical system *except* the secondary-mirror position, over a 24-hour period. It is presumed that the PSF-knowledge requirement will be met by a combination of (a) holding all elements stable to the required accuracy except for secondary mirror and pointing stability; (b) using tracking data to reconstruct pointing motion at few-Hz rate; (c) using stellar images in science data to infer the position of the secondary mirror plus errors in the tracking solution. Strength of the L2 reqs for this strategy is subject to review.

(7) Pursuant to note (7), this is the RMS error in the telemetered pointing history due to measurement error and to vibrations/motion outside the telemetered tracker bandwidth. This figure applies to pitch and yaw; spec on roll is weaker by 1/(maximum field radius of science instruments).

(8) PSF second moments must vary by this much or less across the bandpass of any shape-measurement filter. Exact value TBD, but the (inevitable) diffraction-induced wavelength dependence. Second moments of broadband images due to chromatic centroid shift (lateral color) are also constrained by this specification.

(9) RMS redshift error: applies to both the sparse redshift survey over full WL area, and the deep photo-z calibration redshift survey.

(10) 5-sigma line-flux detection threshold for galaxy with 0.3" half-light radius across whole emission line survey wavelength range.

(11) Fraction of circumscribed survey area of each disjoint field that is imaged in all filters.

FILTER TABLE – Weak Lensing

Filter	F0	F1	F2	F3	F4	F5	F6	F7
Bandpass (nm)	380-460	410-560	500-670	600-810	720-970	860-1170	1040-1410	1250-1700
EE50 radius (mas)	<350	<350	<170	<170	<170	<180	<200	<210
Noise magnitude	>28	>28	>27.6	>27.6	>27.6	>27.3	>27.3	>27.3
Shape data	No	No	Yes	Yes	Yes	No	No	No
Pixel scale	(ground)	(ground)	0.2	0.2	0.2	0.34	0.34	0.34
Exposures			2x2x200s	2x2x200s	2x2x200s	2x200s	2x200s	2x200s

Note 1: These requirements are a point design which attains the *minimum* n_{eff} in L1-1. Many different options are possible. A proposed set of filter bandpasses, EE50's, and noise levels must be checked against a galaxy model to see if L1 requirements are attained.

Note 2: Rows in grey are not requirements; they are an implementation that will reach the requirements with 1.5m telescope, with assumptions for telescope/detector specs.

Appendix B - Integral Field Unit (IFU) Spectrometer

The RM can accommodate an Integral Field Unit (IFU) spectrograph, such as the one that has been prototyped and space-qualified for JDEM by the LAM/Marseille group. The IFU spectrograph was the subject of a recent two-week NASA/Goddard Mission Design Lab (MDL) study and has had substantial oversight from GSFC. Such a spectrograph provides R=75--100 visible-to-infrared spectrophotometry with 100% fill factor for every pixel in a 3 arcseconds by 6 arcseconds FOV at a pixel scale of 0.15 arcseconds per pixel. A complete IFU has been designed to fit within a small 15x15x30 cm volume, with a weight of <12 kg.

There are a number of advantages of spectrophotometry obtained in this way that make the IFU spectrograph particularly attractive: 1) Much faster spectroscopy to reach a given signal-to-noise than slitless or wide-slit alternatives, due to much lower noise. 2) Straightforward flat fielding, wavelength and flux calibration, host galaxy subtraction, and overall spectrophotometric reduction. The format is equivalent to multiple slit

spectra densely packed, so the spatial and spectral information are not entangled. Tested spectrophotometric performance is better than 1% uncertainty. 3) Very large pointing tolerance, including for host galaxy subtraction exposures performed a year later.

4) The IFU exposure times can be tuned to the apparent magnitude of each SN, whereas for multiplex observations with a slitless prism all exposures must reach the maximum target redshift for any given tier (in, e.g., a "layer cake" observing strategy). Since the exposure times increase extremely steeply with redshift (~[1+z]^6), multiplexing is therefore a minor effect in practice. In fact, with t_exp ~[1+z]^6, most of the spectroscopy observing time goes into the very highest redshifts, where there are few (~2) SNe contributing significant signal simultaneously in any field. 5) An IFU spectrograph supports an adaptable SN program that can respond to new knowledge and be tuned to emphasize different SN epochs and different redshift distributions, while avoiding bias against faint SNe.

There are also several advantages for the overall JDEM mission: 6) An IFU spectrograph also acts as the calibration system for JDEM broadband photometry, providing the transfer mechanism from the bright fundamental standard stars to primary and/or secondary standard stars. 7) With an IFU spectrograph, the time used for SN spectroscopy can also be used in parallel to provide Weak Lensing photo-z calibration by observing with the wide-field slitless spectrograph mode simultaneously and building up a very deep set of galaxy spectra using the CCD and HgCdTe imagers.

We note that trade studies have been performed that show a rather simple operations plan can schedule the IFU observations to be slotted into regular observing slots throughout the year, with several weeks of time available to comfortably prepare the entries for a given observing slot. A small percentage (typically <15%) of the supernovae that are near a high-brightness-gradient on the galaxy image are scheduled for a repeat visit after the supernova has faded.

In addition to the speed advantages, the efficiency of the IFU spectrophotometry can make possible detailed spectroscopic characterizations of the SNe that help constrain the SN distance measurement systematics (e.g. due to evolution of SN properties and dust). In particular, the measurements of spectral feature ratios and line velocities require much higher signal-to-noise spectra than the simple identification of Type Ia SNe and redshift determination.

Appendix C - Long Wavelength (2-4 microns) Option

I. Introduction

The goal of all dark energy experiments is to provide data that facilitates a deeper understanding of the source of dark energy. JDEM will have met this goal if it can leave a legacy of precise measures that permit us to answer three fundamental questions:

(1) Is dark energy real, or a manifestation of an incomplete theory of gravity?

(2) If dark energy is real, is it Einstein's cosmological constant – i.e., is w equal to -1?

(3) If dark energy is real, and changes over time and space (e.g., quintessence), then what is its behavior over cosmological time?

The current set of JDEM instruments addresses some, but not all, of these questions. As explained below, conducting a relatively small (1,000 square degree) galaxy survey using a simple all-reflective grating spectrometer capable of measuring the power spectrum between $z = 2$ and 5 ($\Leftrightarrow \lambda = 2\text{-}4$ μm in Hα) would supplement JDEM's capabilities for all of these key questions. Moreover, such a capability makes good use of the low natural background in space, allowing such a survey to exceed the results obtainable from any ground-based experiment.

II. A High-z Survey and the Reality of Dark Energy

Measures of the growth of structure are critical to distinguishing between expansion models driven by dark energy versus models positing a modified form of gravity. The present JDEM relies almost exclusively on weak lensing to provide this information; supernovae and BAO-only provide little-to-no information on the growth of structure. Use of the full power spectrum at $z \leq 2$, including the Alcock-Paczynski test and redshift-space distortions, can provide growth-of-structure measures; however, the need for corrections necessary to compensate for gravitational evolution – so-called non-linear corrections – increases with the passage of cosmic time, i.e., with decreasing redshift..

A 1,000 sq. degree galaxy survey at $2 \leq z \leq 5$ would provide data that would enable highly accurate growth-of-structure measures. Doing so would not only provide a second, independent, measure of this critical quantity, but would also provide an important cross-check of the weak lensing results.

III. A High-z Survey and Einstein's Cosmological Constant

Unfortunately, attempts to understand dark energy based on known physics either fail by many orders of magnitude or require what appears to be arbitrary fine-tuning of initial conditions. At present, such attempts start either with the assumption that dark energy is Einstein's cosmological constant, i.e., $w = -1$, or that w varies with redshift. Distinguishing between these possibilities is a major objective of the JDEM mission (and most ground-based experiments).

A $2 \leq z \leq 5$ galaxy survey can contribute to both the accuracy and confidence of the determination of w in two ways.

First, none of the techniques being considered for JDEM measures dark energy directly. Rather, all techniques measure the expansion rate of the Universe, of which dark energy is but one component (along with the radiation and matter density and curvature). Specifically, the expansion rate as a function of scale factor a is given by the Friedmann equation

$$H^2(a) = H_0^2 \left[\Omega_R a^{-4} + \Omega_M a^{-3} + \Omega_k a^{-2} + \Omega_{DE} \exp\left\{ 3 \int_a^1 \frac{da'}{a'} \left[1 + w(a') \right] \right\} \right],$$

where a =1 at present and is related to redshift by the relation $1 + z = 1/a$, Ω_i is the present fraction of the critical density, $\rho_C = 3H_0^2/8\pi G$, in the form of component i; e.g., radiation (R), matter (M), curvature (k) and dark energy (DE). The parameter H_0 is the present value of the expansion rate of the Universe (Hubble's constant). Finally, $w(a)$ is the ratio of the pressure to the energy density for dark energy, $w(a) = p(a)/\rho(a)$. If Dark Energy is Einstein's cosmological constant, $w(a) = -1$. A $z = 2$ to 5 survey over 1,000 square degree would constrain curvature (Ω_k) to a level more than a factor of 10 better than the current limit of 10^{-2}, thus improving the measure of $H(a)$ by *all* techniques.

Second, if it is found that w is consistent with a value of -1, a $2 \leq z \leq 5$ 1,000 square degree survey would add confidence in this important finding. If $w = -1$, a $2 \leq z \leq 5$ survey would be capable of directly measuring the effects of dark energy out to redshifts between 3 and 4. Confirmation that $w = -1$ obtained using four independent measures at redshifts between 1 and 4 adds confidence in this result beyond three measures between redshifts of 1 and 2.

IV. A High-*z* Survey and a Varying *w*

If the $1 \leq z \leq 2$ techniques should determine that dark energy is not described by Einstein's cosmological constant, i.e., $w \neq -1$, the result would be profound and measuring the variation of w over as broad a redshift range as possible would become indispensable to understanding the source of dark energy. In this instance, extrapolating the value of $w(a)$ from $z < 2$ observations to higher redshifts is questionable, if not dangerous, given the unknown nature of the driving force. Only direct measurements at higher redshifts would suffice. Inclusion of a λ = 2-4 μm spectrometer would provide these data.

V. Uniqueness of λ = 2 to 4 μm Observations

A background-limited, large-area survey would produce data unmatched by any ground-based telescope, for two reasons. First, as shown below, the atmospheric transmission from a high (13,800 ft.), dry (1mm overhead precipitable water vapor) site is generally poor between 2 and 4 microns. A survey that samples all redshifts in this band is thus difficult from the ground.

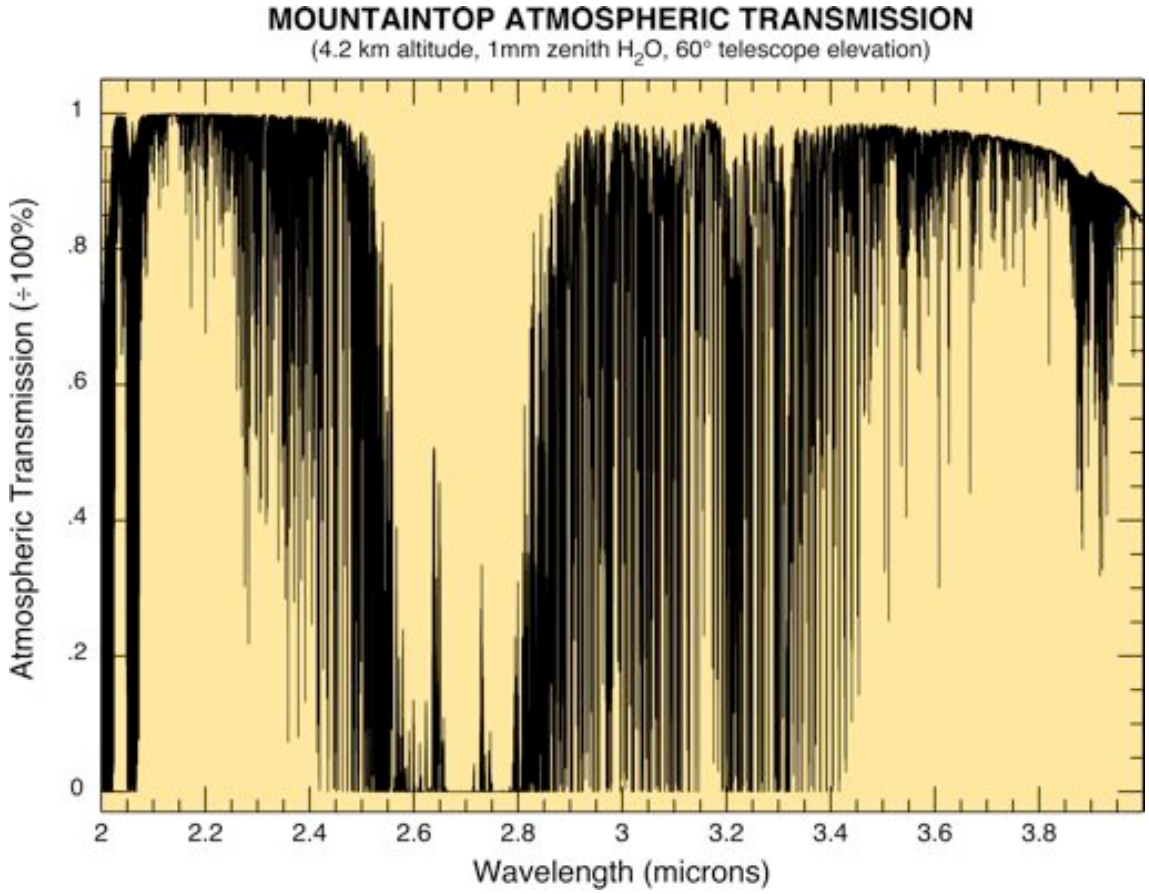

Fig. C1. Atmospheric transmission along a 60°-elevation line of sight from a high (13,800 ft.), dry (1mm precipitable zenith water vapor) site, such as applies to Mauna Kea.

Second, as shown below, even were the atmospheric transmission excellent, the self-generated 2-4 micron infrared background from an ambient temperature (300 K) telescope with 10% emissive optics is between 10^2 and 10^6 times greater than the natural background toward the ecliptic pole. This large difference allows a 1.5-meter space-based aperture, such as JDEM, to significantly exceed the sensitivity of a large ground-based telescope for a given integration time.

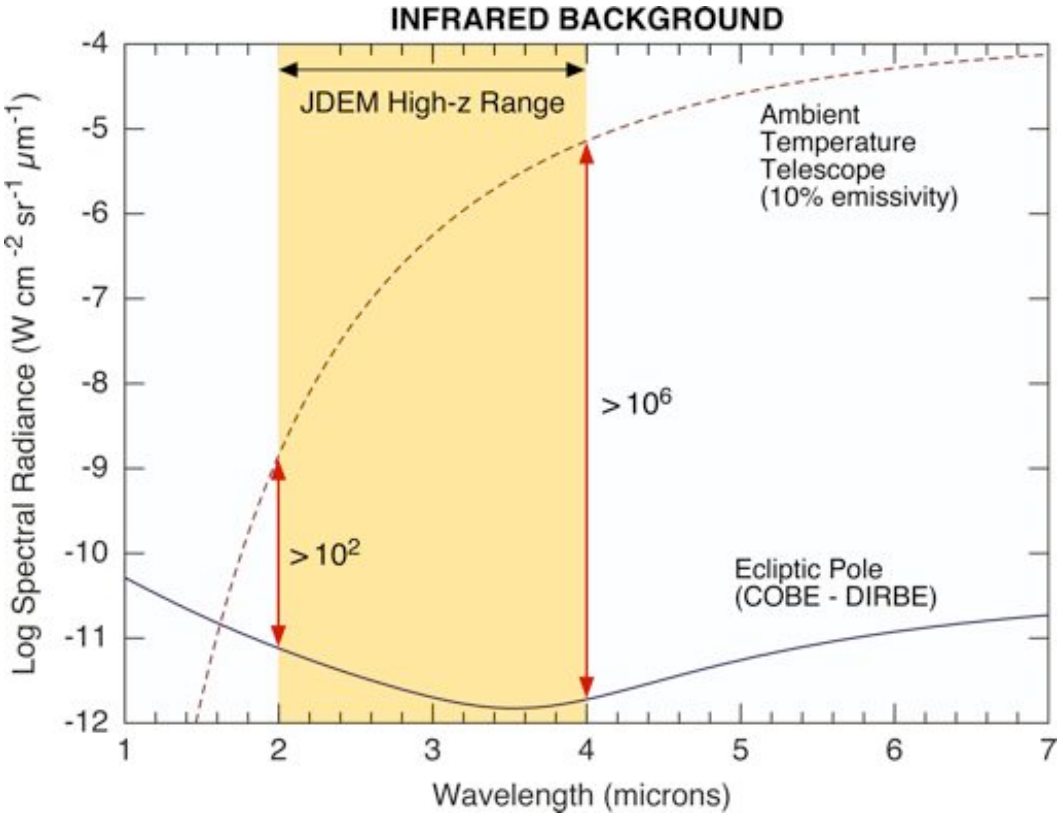

Fig. C2. Infrared background of an ambient temperature (300 K) telescope with mirror emissivities of 10% contrasted with the natural infrared background set by the combination of scattered sunlight and thermal emission from zodiacal dust at the ecliptic pole, where the JDEM survey would be conducted. The zodiacal background at the ecliptic poles has been measured directly by the Infrared Astronomical Satellite (IRAS) and, more recently, by the Diffuse Infrared Background Experiment (DIRBE) aboard the Cosmic Background Explorer (COBE). The curve shown here is a fit to the DIRBE data obtained by Reach (see SIRTF Observatory Performance and Interface Control Document v.3.1, 12 December 2000, p.~30).

VI. Summary

A 1,000 square degree $2 \leq z \leq 5$ galaxy survey would add to DE understanding in 3 important ways. First, such a survey would provide a powerful and independent measure of the growth of structure that would also serve to verify the weak lensing growth-of-structure results. Second, even if the $1 \leq z \leq 2$ techniques reduce the error bars associated with the result that $w = -1$, direct and independent confirmation of this result to a redshift of 3-4 would add significant confidence. In addition, improved measures of space curvature (by more than a factor of 10) possible with a high-z survey would result in reduced uncertainties for *all* $1 \leq z \leq 2$ techniques. Third, if dark energy were found to not be described by Einstein's cosmological constant, a high-z survey would provide indispensible measures of w across a broad range of redshifts. Finally, the science enabled by a 2 to 4 micron survey is beyond the reach of ground-based telescopes.